Metastability in Interacting Nonlinear Stochastic Differential Equations. I: From Weak Coupling to Synchronisation

Nils Berglund, Bastien Fernandez, Barbara Gentz

Metastability in Interacting Nonlinear Stochastic Differential Equations I: From Weak Coupling to Synchronisation

Nils Berglund, Bastien Fernandez and Barbara Gentz

Abstract

We consider the dynamics of a periodic chain of N coupled overdamped particles under the influence of noise. Each particle is subjected to a bistable local potential, to a linear coupling with its nearest neighbours, and to an independent source of white noise. The system shows a metastable behaviour, which is characterised by the location and stability of its equilibrium points. We show that as the coupling strength increases, the number of equilibrium points decreases from 3^N to 3. While for weak coupling, the system behaves like an Ising model with spin-flip dynamics, for strong coupling (of the order N^2), it synchronises, in the sense that all particles assume almost the same position in their respective local potential most of the time. We derive the exponential asymptotics for the transition times, and describe the most probable transition paths between synchronised states, in particular for coupling intensities below the synchronisation threshold. Our techniques involve a centre-manifold analysis of the desynchronisation bifurcation, with a precise control of the stability of bifurcating solutions, allowing us to give a detailed description of the system's potential landscape.

Date. November 21, 2006. Revised version, July 5, 2007.
2000 *Mathematical Subject Classification.* 37H20, 37L60 (primary), 37G40, 60K35 (secondary)
Keywords and phrases. Spatially extended systems, lattice dynamical systems, open systems, stochastic differential equations, interacting diffusions, transitions times, most probable transition paths, large deviations, Wentzell-Freidlin theory, diffusive coupling, synchronisation, metastability, symmetry groups.

1 Introduction

Lattices of interacting deterministic multistable systems display a wide range of interesting behaviours, due to the competition between local dynamics and coupling between different sites. While for weak coupling, they often exhibit spatial chaos (independent dynamics at the different sites), for strong coupling they tend to display an organised collective behaviour, such as synchronisation (see, for instance [BM96, CMPVV96, Joh97, NMKV97], and [PRK01, CF05] for reviews).

An important problem is to understand the effect of noise on such systems. Noise can be used to model the effect of unresolved degrees of freedom, for instance the influence of external heat reservoirs (see, e.g., [FKM65, SL77, EPRB99, RBT00, RBT02]), which can induce currents through the chain. The long-time behaviour of the system is described by its invariant measure (assuming such a measure exists); however, for weak

noise, the dynamics often displays metastability, meaning that the relaxation time towards the invariant measure is extremely long.

Metastability has been studied extensively for particle systems with stochastic dynamics. In these models, the transition from one metastable state to another usually involves the gradual creation of a critical droplet through small fluctuations, followed by a rapid transition to the new state. The distributions of transition times, as well as the shapes of critical droplets, have been investigated in detail (see in particular [dH04, OV05] for reviews, and references therein).

In these lattice models, the local variables take only a finite number of discrete values, which are independent of the interaction with other sites. In the present paper, we consider by contrast a model with continuous on-site variables. This leads to a system of interacting stochastic differential equations (also called interacting diffusions, see, for instance, [DG88] for a review of asymptotic properties in the mean-field case). It turns out that while this system has a similar behaviour to stochastic lattice models for weak coupling, the dynamics is totally different for strong coupling: There are only 3 equilibrium configurations left, while the activation energy becomes extensive in the number N of particles. For large N, the system's behaviour is closer to the behaviour of a Ginzburg–Landau partial differential equation with noise (see, e.g. [EH01, Rou02]). The transition between the strong-coupling and the weak-coupling regimes involves, as we shall see, a sequence of symmetry-breaking bifurcations. Such bifurcations have been studied, for instance, in [QC04] for the weak-coupling regime, and in [McN99, McN02, Wat93a, Wat93b] for systems of coupled phase oscillators.

Our major aim is to determine the dependence of the transition times between metastable states, as well as the critical configurations, on the coupling strength, on the whole range from weak to strong coupling. This analysis requires a precise knowledge of the system's "potential landscape", in particular the number and location of its local minima and saddles of index 1 [FW98, Sug96, Kol00, BEGK04, BGK05]. In order to obtain this information, we will exploit the symmetry properties of the system, using similar techniques as the ones developed in the context of phase oscillators in [AS92, DGS96a, DGS96b], for instance. Our study also involves a centre-manifold analysis of the desynchronisation bifurcation, which goes beyond existing results on similar bifurcations because a precise control of the stability of the bifurcating stationary points is required.

This paper is organised as follows. Section 2 contains the precise description of the model and the statement of all results. After introducing the model and describing its behaviour for weak and strong coupling, in Section 2.5 we examine the effect of symmetries on the bifurcation diagram. A few special cases with small particle number N are illustrated in Section 2.6. The desynchronisation bifurcation for general N is discussed in Section 2.7, while Section 2.8 considers further bifurcations of the origin. Finally, Section 2.9 presents the consequences of these results for the stochastic dynamics of the system.

The subsequent sections contain the proofs of our results. The proof of synchronisation at strong coupling is presented in Section 3, while Section 4 introduces Fourier variables, which are used to prove the results for $N = 2$ and $N = 3$, and for the centre-manifold analysis of the desynchronisation bifurcation for general N. Appendix A gives a brief description of the analysis of the weak-coupling regime, which uses standard techniques from symbolic dynamics, and Appendix B contains a short description of the analysis of the case $N = 4$.

The follow-up work [BFG06b] analyses in more detail the behaviour for large particle number N. In that regime, we are able to control the number of stationary points in a

much larger domain of coupling intensities, including values far from the synchronisation threshold.

Acknowledgements

Financial support by the French Ministry of Research, by way of the *Action Concertée Incitative (ACI) Jeunes Chercheurs, Modélisation stochastique de systèmes hors équilibre*, is gratefully acknowledged. NB and BF thank the Weierstrass Institute for Applied Analysis and Stochastics (WIAS), Berlin, for financial support and hospitality. BG thanks the ESF Programme *Phase Transitions and Fluctuation Phenomena for Random Dynamics in Spatially Extended Systems (RDSES)* for financial support, and the Centre de Physique Théorique (CPT), Marseille, for kind hospitality.

2 Model and Results

2.1 Definition of the Model

In our study of the influence of noise on lattice dynamical systems with continuous on-site variables, we shall focus on a model which can serve as a paradigm for such systems. It is based on coupled bistable ordinary differential equations governed by the competition between individual effects and spatial interactions. To name a few examples, it applies for instance to chains of particles placed in a quartic potential and coupled by springs [FM96], to stimulus conduction in the myocardial tissue [Kee87] and to certain chemical reactions [EN93]. Another motivation for choosing this specific model is that it allows for a quantitative description of phenomena, while being generic. In particular, it quantifies changes from intensive to extensive properties when the interaction strength increases.

The system is defined by the following ingredients:

- The periodic one-dimensional lattice is given by $\Lambda = \mathbb{Z}/N\mathbb{Z}$, where $N \geqslant 2$ is the number of particles.
- To each site $i \in \Lambda$, we attach a real variable $x_i \in \mathbb{R}$, describing the position of the ith particle. The configuration space is thus $\mathcal{X} = \mathbb{R}^{\Lambda}$.
- Each particle feels a local bistable potential, given by

$$U(\xi) = \frac{1}{4}\xi^4 - \frac{1}{2}\xi^2 , \qquad \xi \in \mathbb{R} . \tag{2.1}$$

  The local dynamics thus tends to push the particle towards one of the two stable positions $\xi = 1$ or $\xi = -1$. The reason for this choice is that $U(\xi)$ is the simplest possible double-well potential, which will be responsible for metastability. Nevertheless, we expect this potential to yield a behaviour which is, to a certain extent, generic among models in its symmetry class.
- Neighbouring particles in Λ are coupled via a discretised-Laplacian interaction, of intensity $\gamma/2$. Such a nearest-neighbour coupling can be expected to yield very different dynamics than mean-field models, for instance.
- Each site is coupled to an independent source of noise, of intensity σ. The sources of noise are described by independent Brownian motions $\{B_i(t)\}_{t\geqslant 0}$.

The system is thus described by the following set of coupled stochastic differential equations, defining a diffusion on $\mathcal{X}$:

$$\mathrm{d}x_i^\sigma(t) = f(x_i^\sigma(t))\,\mathrm{d}t + \frac{\gamma}{2}\big[x_{i+1}^\sigma(t) - 2x_i^\sigma(t) + x_{i-1}^\sigma(t)\big]\,\mathrm{d}t + \sigma\,\mathrm{d}B_i(t)\;, \qquad i \in \Lambda\;, \tag{2.2}$$

where the local nonlinear drift is given by

$$f(\xi) = -\nabla U(\xi) = \xi - \xi^3\;. \tag{2.3}$$

For $\sigma = 0$, the system (2.2) is a gradient system of the form $\dot{x} = -\nabla V_\gamma(x)$, with potential

$$V_\gamma(x) = \sum_{i\in\Lambda} U(x_i) + \frac{\gamma}{4}\sum_{i\in\Lambda}(x_{i+1} - x_i)^2\;. \tag{2.4}$$

Note that the local potential $U(\xi)$ is invariant under the transformation $\xi \mapsto -\xi$, implying that the local dynamics has no preference for either positive or negative ξ. An interesting question is how the results are affected by adding a symmetry-breaking term to $U(\xi)$. This question will be the subject of future research. Some preliminary studies indicate that several results, such as the presence of synchronisation for strong coupling, the structure of the desynchronisation bifurcation, and the qualitative behaviour for weak coupling, are not much affected by the asymmetry. However, many details of the bifurcation diagrams, as well as the metastable timescales and transition paths, will of course be quite different.

2.2 Potential Landscape and Metastability

The dynamics of the stochastic system depends essentially on the "potential landscape" V_γ. More precisely, let

$$\mathcal{S} = \mathcal{S}(\gamma) = \{x \in \mathcal{X}\colon \nabla V_\gamma(x) = 0\} \tag{2.5}$$

denote the set of stationary points of the potential. A point $x \in \mathcal{S}$ is said to be of type (n_-, n_0, n_+) if the Hessian matrix of V_γ at x has n_- negative, n_+ positive and $n_0 = N - n_- - n_+$ vanishing eigenvalues (counting multiplicity). For each $k = 0, \dots, N$, let $\mathcal{S}_k = \mathcal{S}_k(\gamma)$ denote the set of stationary points $x \in \mathcal{S}$ which are of type $(k, 0, N-k)$. For $k \geqslant 1$, these points are called *saddles of index* k, or simply *k-saddles*, while $\mathcal{S}_0$ is the set of strict local minima of V_γ.

The stochastic system (2.2) admits an invariant probability measure with density proportional to $\mathrm{e}^{-2V_\gamma(x)/\sigma^2}$, implying that asymptotically, the system spends most of the time near the deepest minima of V_γ. However, the invariant measure does not contain any information on the dynamics between these minima, nor on the way the equilibrium distribution is approached. Loosely speaking, for small noise intensity σ the stochastic system behaves in the following way [FW98]:

- A sample path $\{x^\sigma(t)\}_t$, starting in a point x_0 belonging to the deterministic basin of attraction $\mathcal{A}(x^\star)$ of a stationary point $x^\star \in \mathcal{S}_0$, will first reach a small neighbourhood of $x^\star$, in a time close to the time it would take a deterministic solution to do so.
- During an exponentially long time span, $x^\sigma(t)$ remains in $\mathcal{A}(x^\star)$, spending most of that time near $x^\star$, but making occasional excursions away from the stationary point.
- Sooner or later, $x^\sigma(t)$ makes a transition to (the neighbourhood of) another stationary point $y^\star \in \mathcal{S}_0$. During this transition, the sample path is likely to pass close to a saddle $s \in \mathcal{S}_1$, whose unstable manifolds converge to $x^\star$ and $y^\star$. In fact, the whole sample path during the transition is likely to remain close to these unstable manifolds.

- After a successful transition, the sample path again spends an exponentially long time span in the basin of $y^\star$, until a similar transition brings it to another point of $\mathcal{S}_0$ (which may or may not be different from $x^\star$).

If we ignore the excursions of the sample paths inside domains of attraction, and consider only the transitions between local minima of the potential, the stochastic process resembles a Markovian jump process on $\mathcal{S}_0$, with exponentially small transition probabilities, the only relevant transitions being those between potential minima connected by a 1-saddle.

Understanding the dynamics for small noise thus essentially requires knowing the graph $\mathcal{G} = (\mathcal{S}_0, \mathcal{E})$, in which two vertices $x^\star, y^\star \in \mathcal{S}_0$ are connected by an edge $e \in \mathcal{E}$ if and only if there is a 1-saddle $s \in \mathcal{S}_1$ whose unstable manifolds converge to $x^\star$ and $y^\star$. The mean transition time from $x^\star$ to $y^\star$ is of order e^{2H/σ^2}, where H is the potential difference between $x^\star$ and the lowest saddle leading from $x^\star$ to $y^\star$.

In our case, the potential $V_\gamma(x)$ being a polynomial of degree 4 in N variables, the set $\mathcal{S}$ of stationary points admits at most 3^N elements. On the other hand, it is easy to see that $\mathcal{S}$ always contains at least the three points

$$O = (0, \dots, 0) \;, \qquad I^\pm = \pm(1, \dots, 1) \;. \tag{2.6}$$

Depending on the value of γ, the origin O can be an N-saddle, or a k-saddle for any odd k. The points $I^\pm$ always belong to $\mathcal{S}_0$, in fact we have for all $\gamma > 0$

$$V_\gamma(x) > V_\gamma(I^+) = V_\gamma(I^-) = -\frac{N}{4} \quad \forall x \in \mathcal{X} \setminus \{I^-, I^+\} \;. \tag{2.7}$$

Thus I^- and I^+ are the most stable configurations of the system, and also the local minima between which transitions take the longest time.

Among the many questions we can ask for the stochastic system, we shall concentrate on the following:

- How long does the system typically take to make a transition from I^- to I^+, and how does the transition time depend on coupling strength γ and noise intensity σ?
- How do typical paths for such a transition look like?

2.3 Weak-Coupling Regime

In the uncoupled case $\gamma = 0$, we simply have

$$\mathcal{S}(0) = \{-1, 0, 1\}^\Lambda \;, \qquad |\mathcal{S}(0)| = 3^N \;. \tag{2.8}$$

Furthermore, $\mathcal{S}_k(0)$ is the set of stationary points having exactly k coordinates equal to 0 (thus $|\mathcal{S}_k(0)| = \binom{N}{k} 2^{N-k}$). In particular, $\mathcal{S}_0(0) = \{-1, 1\}^\Lambda$ has cardinality 2^N.

Hence the graph $\mathcal{G}$ is an N-dimensional hypercube: Two vertices $x^\star$, $y^\star \in \mathcal{S}_0(0)$ are connected if and only if they differ in exactly one component. Note that $V_0(x^\star) = -N/4$ for all local minima $x^\star$, and $V_0(s) = -(N-1)/4$ for all 1-saddles s, implying that all nearest-neighbour transitions of the uncoupled system take the same time (of order $\mathrm{e}^{1/2\sigma^2}$) on average.

For small positive coupling intensity $0 < \gamma \ll 1$, the implicit-function theorem guarantees that all stationary points depend analytically on γ, without changing their type. In addition, the following result is a direct consequence of standard results on Hénon-like mappings of the plane:

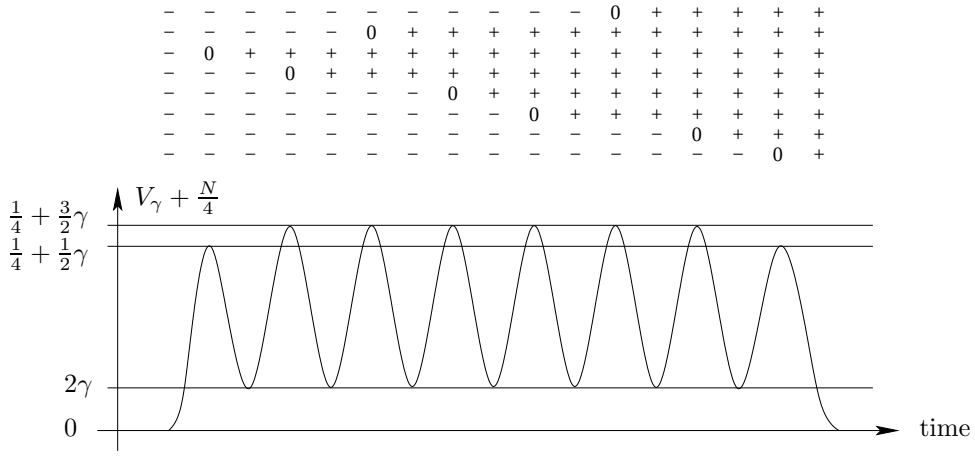

FIGURE 1. Example of an optimal transition path from I^- to I^+ for weak coupling. The upper half of the figure shows the local minima and 1-saddles visited during the transition, displayed vertically. For instance, the second column means that the first 1-saddle visited is a perturbation of order γ of the stationary point $(-1,-1,0,-1,-1,-1,-1,-1)$ present in absence of coupling. The lower half of the figure shows the value of the potential seen along the transition path.

Proposition 2.1. *For any N, there exists a critical coupling $\gamma^\star(N)$ such that for all $0 \leqslant \gamma < \gamma^\star(N)$, the stationary points $x^\star(\gamma) \in \mathcal{S}(\gamma)$ depend continuously on γ, without changing their type. The critical coupling $\gamma^\star(N)$ satisfies*

$$\inf_{N \geqslant 2} \gamma^\star(N) > \frac{1}{4} \,. \tag{2.9}$$

The proof is briefly discussed in Appendix A, where we also provide slightly better lower bounds on $\inf_{N\geqslant 2}\gamma^\star(N)$. We expect the critical coupling to be quite close to $1/4$, however. In particular, we will show below that $\gamma^\star(2) = 1/3$, $\gamma^\star(3) = 0.2701\ldots$, and $\gamma^\star(4) = 0.2684\ldots$

Since any stationary point $x^\star(\gamma) = (x_1^\star(\gamma), \ldots, x_N^\star(\gamma)) \in \mathcal{S}(\gamma)$ satisfies $x^\star(\gamma) = x^\star(0) + \mathcal{O}(\gamma)$, where each $x_i^\star(0)$ is a stationary point of the local potential U, one has

$$\begin{aligned} V_\gamma(x^\star(\gamma)) &= V_\gamma(x^\star(0)) + \mathcal{O}(\gamma^2) \\ &= V_0(x^\star(0)) + \frac{\gamma}{4}\sum_{i=1}^{N}(x_{i+1}^\star(0) - x_i^\star(0))^2 + \mathcal{O}(\gamma^2) \,. \end{aligned} \tag{2.10}$$

To first order in γ, the potential's increase due to coupling depends on the number of interfaces in the unperturbed configuration $x^\star(0) \in \mathcal{S}(0)$ (recall from (2.8) that the components of $x^\star(0)$ only take values in $\{-1,0,1\}$). The dynamics of the stochastic system is thus essentially the one of an Ising-spin system with Glauber dynamics. Starting from the configuration I^-, the system reaches with equal probability any configuration with one positive and $N-1$ negative spins. Then, however, it is less expensive to switch a spin neighbouring the positive one than to switch a far-away spin, which would create more interfaces. Thus the optimal transition from I^- to I^+ consists in the growth of a "droplet of $+$ in a sea of $-$" (Figure 1). To first order in the coupling intensity, all visited 1-saddles except the first and last one have the same potential value $-N/4 + 1/4 + (3/2)\gamma + \mathcal{O}(\gamma^2)$.

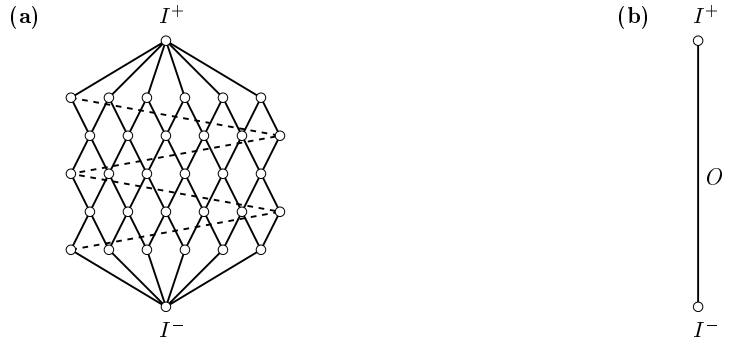

FIGURE 2. **(a)** Structure of the graph $\mathcal{G}$ in the small-coupling regime $0 < \gamma < \gamma^\star(N)$. Only edges belonging to optimal paths are shown: In the Ising-model analogy, these paths correspond to the flip of neighbouring spins. **(b)** The graph $\mathcal{G}$ in the synchronisation regime $\gamma > \gamma_1(N)$.

The energy required for the transition is thus

$$V_\gamma\big((-1,-1,\dots,-1,0,1,1,\dots,1) + \mathcal{O}(\gamma)\big) - V_\gamma\big(I^-\big) = \frac{1}{4} + \frac{3}{2}\gamma + \mathcal{O}(\gamma^2)\,, \tag{2.11}$$

which is independent of the system size. Note that the situation is different for lattices of dimension larger than 1, in which the energy increases with the surface of the droplet (cf. [dH04]).

2.4 Synchronisation Regime

For strong coupling γ, the situation is completely different than for weak coupling. Indeed, we have the following result (see Section 3 for the proof):

Proposition 2.2. *Let*

$$\gamma_1 = \gamma_1(N) = \frac{1}{1-\cos(2\pi/N)} = \frac{N^2}{2\pi^2}\left[1 - \mathcal{O}\left(\frac{1}{N^2}\right)\right]. \tag{2.12}$$

Then $\mathcal{S}(\gamma) = \{O, I^+, I^-\}$ if and only if $\gamma \geqslant \gamma_1$. Moreover, the origin O is a 1-saddle if and only if $\gamma > \gamma_1$, and in that case its unstable manifold is contained in the diagonal

$$\mathcal{D} = \{x \in \mathcal{X} \colon x_1 = x_2 = \cdots = x_N\}\,. \tag{2.13}$$

We say that the deterministic system is *synchronised* for $\gamma > \gamma_1$, in the sense that the diagonal is approached as $t \to \infty$ for any initial state, meaning that all coordinates x_i are asymptotically equal. In other words, the system behaves as if all particles coagulate in order to form one large particle of mass N. The graph $\mathcal{G}$ contains only two vertices $I^\pm$, connected by a single edge (Figure 2b). By extension, in the stochastic case we will say that the system is synchronised whenever all coordinates x_i^σ remain close to each other most of the time with high probability. Then transitions between I^- and I^+ occur in a small neighbourhood of the diagonal.

In this case, the energy required for the transition is

$$V_\gamma(O) - V_\gamma\big(I^-\big) = \frac{N}{4}\,, \tag{2.14}$$

which is extensive in the system size. Transitions now take a time of order $\mathrm{e}^{N/2\sigma^2}$, and are thus much less frequent in the synchronisation regime than in the low-coupling regime.

It is remarkable that as the coupling γ grows from 0 to γ_1, the number of stationary points decreases from 3^N to 3. The main purpose of this work is to elucidate in which way this transition occurs, and how it affects the transition paths and times.

2.5 Symmetry Groups

The deterministic system $\dot{x} = -\nabla V_\gamma(x)$ is equivariant (that is, $\nabla V_\gamma(gx) = g\nabla V_\gamma(x)$ for all $x \in \mathcal{X}$) under three different types of symmetries g:

- Cyclic permutations (corresponding to rotations around the diagonal), generated by
$$R(x_1, \dots, x_N) = (x_2, \dots, x_N, x_1) \,, \tag{2.15}$$
as a consequence of the particles being identical.
- Reflection symmetries $R^k S$, $k = 0, \dots, N-1$, where
$$S(x_1, \dots, x_N) = (x_N, x_{N-1}, \dots, x_1) \,, \tag{2.16}$$
as a consequence of the interaction being isotropic.
- The inversion
$$C(x_1, \dots, x_N) = -(x_1, \dots, x_N) \,, \tag{2.17}$$
as a consequence of the local potential being even.

The symmetries R and S generate the dihedral group D_N, which has order $2N$, for $N \geqslant 3$, and the group $\mathbb{Z}_2$ for $N = 2$. For $N \geqslant 3$, the symmetries R, S and C generate a group of order $4N$, which we shall denote $G = G_N = D_N \times \mathbb{Z}_2$. For $N = 2$ the symmetry group is the Klein four-group $G_2 = \mathbb{Z}_2 \times \mathbb{Z}_2$, which as order 4.

The set of stationary points $\mathcal{S}(\gamma)$, as well as each set $\mathcal{S}_k(\gamma)$ of k-saddles, are invariant under G. Thus G acts as a group of transformations on $\mathcal{X}$, on $\mathcal{S}(\gamma)$, and on each $\mathcal{S}_k(\gamma)$. We will use a few concepts from elementary group theory:

- For $x \in \mathcal{X}$, the *orbit* of x is the set $O_x = \{gx \colon g \in G\}$.
- For $x \in \mathcal{X}$, the *isotropy group* or *stabiliser* of x is the set $C_x = \{g \in G \colon gx = x\}$.
- The *fixed-point set* of a subgroup H of G is the set $\mathrm{Fix}(H) = \{x \in \mathcal{X} \colon hx = x \; \forall h \in H\}$.

The following facts are well known:

- For any x, the isotropy group C_x is a subgroup of G and $|C_x||O_x| = |G|$ (where $|X|$ denotes the cardinality of a finite set X).
- For any $g \in G$ and $x \in \mathcal{X}$, we have $C_{gx} = gC_xg^{-1}$, so that the isotropy groups of all the points of a given orbit are conjugate.
- For any subgroup H of G and any $g \in G$, $\mathrm{Fix}(gHg^{-1}) = g\,\mathrm{Fix}(H)$.

These facts allow us to limit the study to one point of each orbit, to one subgroup in each conjugacy class, and to one type of conjugated fixed-point set. For small N, this reduction often suffices to completely determine all stationary points of the system, while for larger N, it at least helps to classify the stationary points.

2.6 Small Lattices

We now consider some particular cases for illustration. The following applies to the three stationary points that are always present:

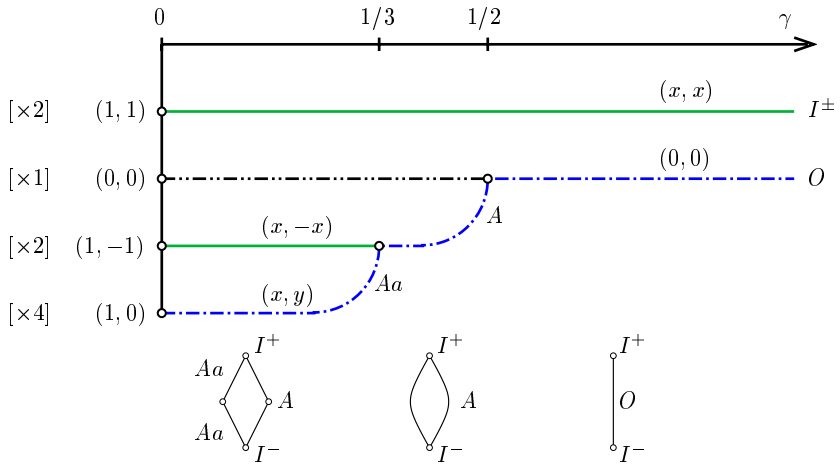

FIGURE 3. Bifurcation diagram for the case $N = 2$ and associated graphs $\mathcal{G}$. Only one stationary point is shown for each orbit of the symmetry group G. The cardinality of the orbit is shown in square brackets. Full lines represent local minima of the potential, while dash–dotted lines with k dots represent k-saddles.

$z^\star$	$O_{z^\star}$	$C_{z^\star}$	$\mathrm{Fix}(C_{z^\star})$
$(0,0)$	$\{(0,0)\}$	$G_2 = \mathbb{Z}_2 \times \mathbb{Z}_2$	$\{(0,0)\}$
$(1,1)$	$\{(1,1),(-1,-1)\}$	$\mathbb{Z}_2 = \{\mathrm{id}, S\}$	$\{(x,x)\}_{x\in\mathbb{R}} = \mathcal{D}$
$(1,-1)$	$\{(1,-1),(-1,1)\}$	$\{\mathrm{id}, CS\}$	$\{(x,-x)\}_{x\in\mathbb{R}}$
$(1,0)$	$\{\pm(1,0),\pm(0,1)\}$	$\{\mathrm{id}\}$	$\{(x,y)\}_{x,y\in\mathbb{R}} = \mathcal{X}$

TABLE 1. Stationary points $z^\star \in \mathcal{S}(0)$, their orbits, their isotropy groups and the corresponding fixed-point sets in the case $N = 2$.

- For the origin O, $O_O = \{O\}$, $C_O = G$ and $\mathrm{Fix}(C_O) = \{O\}$.
- For the global minima $I^\pm$, $O_{I^+} = O_{I^-} = \{I^-, I^+\}$, $C_{I^\pm} = D_N$ and $\mathrm{Fix}(C_{I^\pm}) = \mathcal{D}$, where $\mathcal{D}$ is the diagonal defined in (2.13).

Case $N = 2$

For $N = 2$, we have $R = S$ and the symmetry group is $G_2 = \{\mathrm{id}, S, C, CS\}$. In the uncoupled case, the set of stationary points $\mathcal{S}(0)$ is partitioned into four orbits, as shown in Table 1. Figure 3 indicates how the stationary points evolve as the coupling increases (the proof is given in Proposition 4.2). We see that stationary points keep the same type of symmetry as the coupling strength γ increases, and sometimes merge with a stationary point of higher symmetry.

Below the bifurcation diagram, we show how the corresponding graphs $\mathcal{G}$ change as the coupling intensity γ varies. The two-dimensional hypercube (i.e., the square), present for weak coupling, transforms into a graph with two vertices, connected by two edges, as the 1-saddles labelled Aa undergo a pitchfork bifurcation at $\gamma = 1/3 = \gamma^\star(2)$. For $1/3 < \gamma < 1/2$, the points with $(x,-x)$-symmetry, labelled A, are 1-saddles, representing the points of maximal potential height on the two optimal transition paths from I^- to I^+. At $\gamma = 1/2 = \gamma_1(2)$, the 1-saddles undergo another pitchfork bifurcation, this time with the origin O, which becomes the only transition gate in the strong-coupling regime.

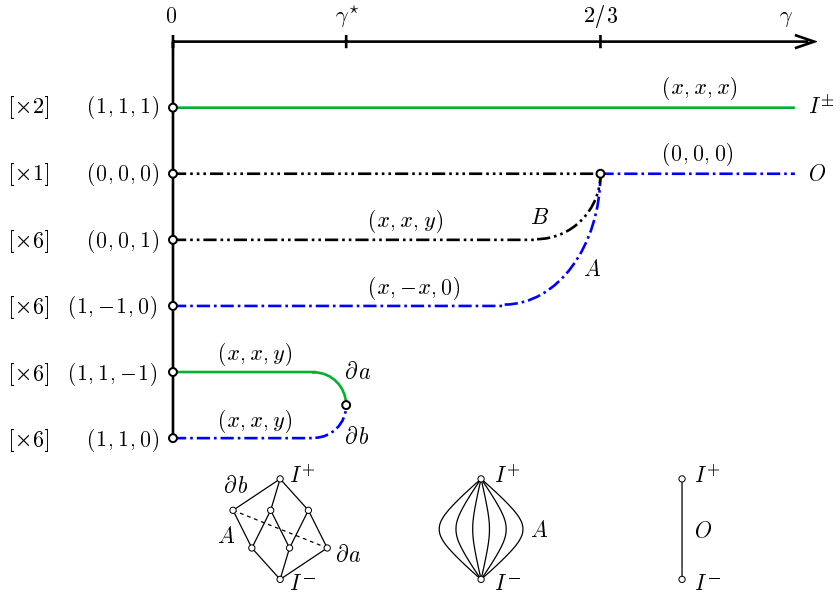

FIGURE 4. Bifurcation diagram for the case $N = 3$ and associated graphs $\mathcal{G}$. Only one stationary point is shown for each orbit of the symmetry group G. The saddle–node bifurcation value is $\gamma^\star = \gamma^\star(3) = (\sqrt{3+2\sqrt{3}} - \sqrt{3})/3 = 0.2701\ldots$

$z^\star$	$O_{z^\star}$	$C_{z^\star}$	$\mathrm{Fix}(C_{z^\star})$
$(0,0,0)$	$\{(0,0,0)\}$	G_3	$\{(0,0,0)\}$
$(1,1,1)$	$\{(1,1,1),(-1,-1,-1)\}$	D_3	$\{(x,x,x)\}_{x\in\mathbb{R}} = \mathcal{D}$
$(1,-1,0)$	$\{\pm(1,-1,0),\pm(-1,0,1),\pm(0,1,-1)\}$	$\{\mathrm{id}, CRS\}$	$\{(x,-x,0)\}_{x\in\mathbb{R}}$
$(0,0,1)$	$\{\pm(0,0,1),\pm(0,1,0),\pm(1,0,0)\}$	$\{\mathrm{id}, RS\}$	$\{(x,x,y)\}_{x,y\in\mathbb{R}}$
$(1,1,-1)$	$\{\pm(1,1,-1),\pm(1,-1,1),\pm(-1,1,1)\}$	$\{\mathrm{id}, RS\}$	$\{(x,x,y)\}_{x,y\in\mathbb{R}}$
$(1,1,0)$	$\{\pm(1,1,0),\pm(1,0,1),\pm(0,1,1)\}$	$\{\mathrm{id}, RS\}$	$\{(x,x,y)\}_{x,y\in\mathbb{R}}$

TABLE 2. Stationary points $z^\star \in \mathcal{S}(0)$, their orbits, their isotropy groups and the corresponding fixed-point sets in the case $N = 3$.

The value of the potential on the bifurcating branches is found to be

$$V_\gamma(A) = -\frac{1}{2}(1-2\gamma)^2\ ,$$
$$V_\gamma(Aa) = -\frac{1}{2}(1-2\gamma)^2 + \frac{1}{4}(1-3\gamma)^2\ . \tag{2.18}$$

Thus in the case $\gamma < 1/3 = \gamma^\star(2)$, the typical time for a transition from I^- to I^+ will be of order $\mathrm{e}^{(1+2\gamma+\gamma^2)/2\sigma^2}$, while for $1/3 < \gamma < 1/2$, it is of order $\mathrm{e}^{4\gamma(1-\gamma)/\sigma^2}$, and for $\gamma > 1/2$ it is of order e^{1/σ^2}.

Case $N = 3$

For $N = 3$, at zero coupling the set $\mathcal{S}(0)$ of stationary points is partitioned into six orbits, as shown in Table 2. Their evolution as the coupling increases is shown in Figure 4 (for a proof, see Proposition 4.3). The new feature in this case is that two orbits disappear

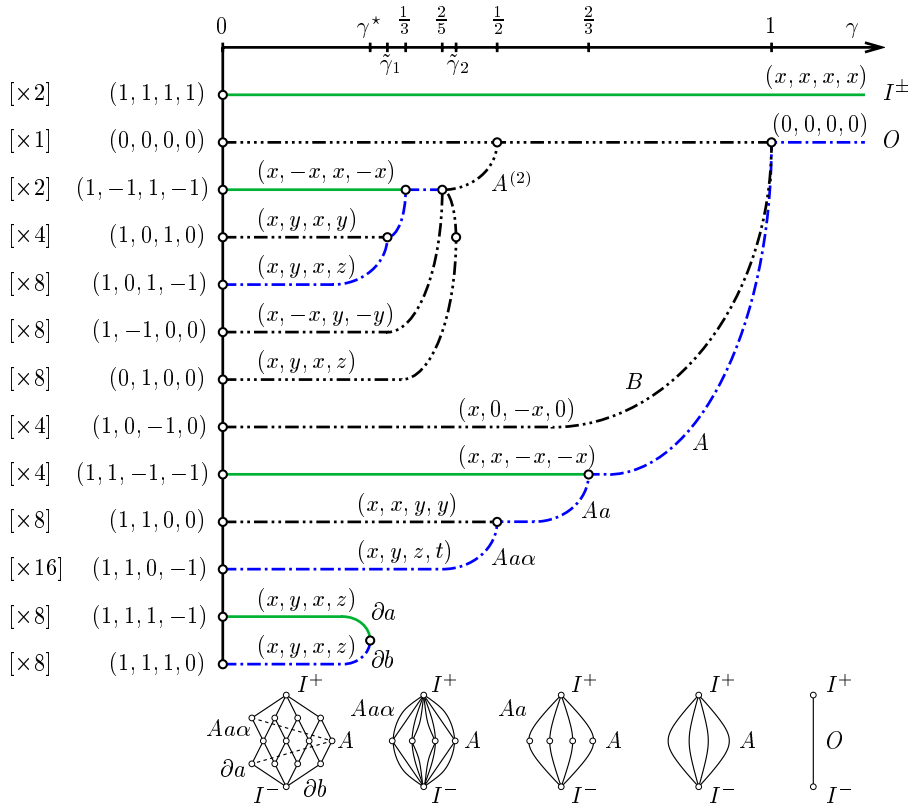

FIGURE 5. Bifurcation diagram for the case $N = 4$ and associated graphs $\mathcal{G}$ (only edges corresponding to optimal transition paths are shown). Only one stationary point is shown for each orbit of the symmetry group G. The saddle–node bifurcation values are $\gamma^\star = \gamma^\star(4) = 0.2684\ldots$ and $\tilde\gamma_2 = 0.4004\ldots$, while $\tilde\gamma_1 = (3\sqrt{2} - 2)/7 = 0.3203\ldots$

in a saddle–node bifurcation at $\gamma = \gamma^\star(3) = (\sqrt{3 + 2\sqrt{3}} - \sqrt{3})/3 = 0.2701\ldots$, instead of merging with stationary points of higher symmetry. This accounts for the rather drastic transformation of the graph $\mathcal{G}$ from a 3-cube for $\gamma < \gamma^\star(3)$ to a graph with two vertices joined by 6 edges for $\gamma^\star(3) < \gamma < 2/3 = \gamma_1(3)$. The potential on the A-branches has value

$$V_\gamma(A) = -\frac{1}{2}\Big(1 - \frac{3}{2}\gamma\Big)^2 . \tag{2.19}$$

Thus in the case $\gamma < 2/3$, the typical time for a transition from I^- to I^+ will be of order $\mathrm{e}^{(2+12\gamma-9\gamma^2)/4\sigma^2}$, while for $\gamma > 2/3$ it is of order $\mathrm{e}^{3/2\sigma^2}$.

Case $N = 4$

Figure 5 shows the results of a similar analysis for $N = 4$. The determination of this bifurcation diagram, which relies partly on the numerical study of the roots of some polynomials, is outlined in Appendix B. As in the previous cases, a certain number of stationary points emerge from the origin as the coupling intensity decreases below the synchronisation threshold. In the present case, the desynchronisation bifurcation occurs at $\gamma = \gamma_1(4) = 1$, and there are four 1-saddles, labelled A, and four 2-saddles, labelled B, emerging from the origin. Two more symmetry-breaking bifurcations affect the A-branches, finally resulting in 1-saddles without any symmetry. A second branch, labelled $A^{(2)}$, bifurcates from the origin at $\gamma = 1/2$. We do not show the corresponding stationary

points in the graphs, because they appear always to correspond to non-optimal transition paths.

The examples discussed here give some flavour of how the transition from weak coupling to synchronisation occurs in the general case. In the sequel, we will mainly describe the desynchronisation bifurcation occurring at $\gamma = \gamma_1(N)$, which can be analysed for arbitrary N.

2.7 Desynchronisation Bifurcation

In this section, we consider the behaviour for general particle number $N \geqslant 3$, and coupling intensities γ slightly below the synchronisation threshold $\gamma_1(N)$. Our aim is to obtain precise information on

- the exact number and stability type of stationary points;
- the potential difference between global minima and saddles of index 1, which governs the transition time between these minima;
- the spatial shape of the critical configurations (i.e., the saddles of index 1), which are the highest energy configurations reached during a typical transition.

Even particle number

We start by considering the case of even particle number N. The main result is the following theorem, which will be proved in Section 4.3.

Theorem 2.3 (Desynchronisation bifurcation, even particle number). *Assume that N is even. Then there exist $\delta = \delta(N) > 0$ and points $A = A(\gamma)$ and $B = B(\gamma)$ in $\mathcal{X}$ such that for $\gamma_1 - \delta < \gamma < \gamma_1$, the set of stationary points $\mathcal{S}(\gamma)$ has cardinality $2N + 3$, and can be decomposed as follows:*

$$\begin{aligned} \mathcal{S}_0 &= O_{I^+} = \{I^+, I^-\} \,, \\ \mathcal{S}_1 &= O_A = \{A, RA, \dots, R^{N-1}A\} \,, \\ \mathcal{S}_2 &= O_B = \{B, RB, \dots, R^{N-1}B\} \,, \\ \mathcal{S}_3 &= O_O = \{O\} \,. \end{aligned} \tag{2.20}$$

Furthermore, the value $V_\gamma(A)$ of the potential is the same on all 1-saddles, and is determined by

$$\frac{V_\gamma(A)}{N} = \begin{cases} -\dfrac{1}{4}(1-\gamma)^2 & \text{if } N = 4 \,, \\ -\dfrac{1}{6}\bigl(1-\gamma/\gamma_1\bigr)^2 + \mathcal{O}\bigl((1-\gamma/\gamma_1)^3\bigr) & \text{if } N \geqslant 6 \,, \end{cases} \tag{2.21}$$

This result tells us that as the coupling intensity γ decreases below the synchronisation threshold γ_1, there are exactly N saddles of index 1 and N saddles of index 2 bifurcating from the origin. All saddles of the same index belong to the same orbit of the symmetry group G. In fact, if the location of one saddle is known, the locations of all other saddles of the same type are obtained by cyclic permutation of its coordinates.

Relation (2.21) shows that the height of the 1-saddles decreases as the coupling intensity γ decreases. A simple topological argument shows that the unstable manifolds of each 1-saddle converge to I^+ and I^-. Thus the transition time from I^- to I^+ will be governed by the potential difference $V_\gamma(A) - V_\gamma(I^-)$.

N	x	C_x	$\mathrm{Fix}(C_x)$
$4L$	A	$\overline{D}_2$	$(x_1,\dots,x_L,x_L,\dots,x_1,-x_1,\dots,-x_L,-x_L,\dots,-x_1)$
	B	$\overline{D}_2'$	$(x_1,\dots,x_L,\dots,x_1,0,-x_1,\dots,-x_L,\dots,-x_1,0)$
$4L+2$	A	$\overline{D}_2$	$(x_1,\dots,x_{L+1},\dots,x_1,-x_1,\dots,-x_{L+1},\dots,-x_1)$
	B	$\overline{D}_2'$	$(x_1,\dots,x_L,x_L\dots,x_1,0,-x_1,\dots,-x_L,-x_L,\dots,-x_1,0)$
$2L+1$	A	$\langle CRS\rangle$	$(x_1,\dots,x_L,-x_L,\dots,-x_1,0)$
	B	$\langle RS\rangle$	$(x_1,\dots,x_L,x_L,\dots,x_1,x_0)$

TABLE 3. Symmetries of the stationary points bifurcating from the origin at $\gamma=\gamma_1$. Here L denotes an integer such that $N=4L$, $N=4L+2$, or $N=2L+1$ depending on the value of N (mod 4). The isotropy groups for even N are $\overline{D}_2=\langle CS,R^{N/2}S\rangle$ and $\overline{D}_2'=\langle CRS,R^{N/2+1}S\rangle$, where $\langle g_1,\dots,g_m\rangle$ denotes the group generated by $\{g_1,\dots,g_m\}$.

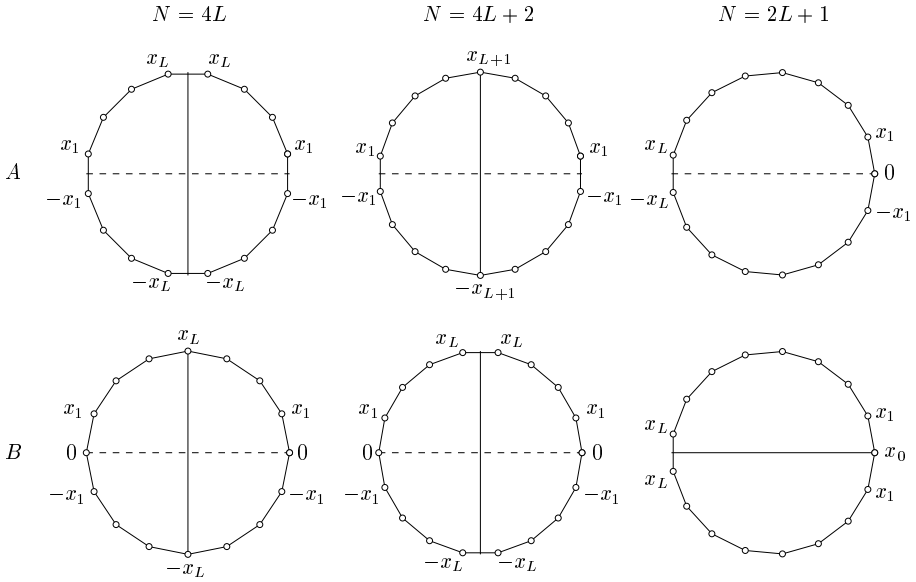

FIGURE 6. Symmetries of the stationary points A and B bifurcating from the origin at $\gamma=\gamma_1$. Full lines represent symmetry axes, broken lines represent symmetry axes with sign change.

Remark 2.4. The proof of Theorem 2.3 actually yields more precise information on the coordinates of the saddles A and B, which can be summarised as follows.

- The saddles A and B satisfy special symmetries, as shown in Table 3 and Figure 6. Namely, their coordinates admit a mirror symmetry, as well as a mirror symmetry with sign change, the two symmetry axes being perpendicular. The details depend on whether $N\in 4\mathbb{N}$ or $N\in 4\mathbb{N}+2$, because this affects the number of coordinates which may lie on the symmetry axes.
- The value $V_\gamma(B)$ of the potential on the 2-saddles satisfies

$$0<\frac{V_\gamma(B)-V_\gamma(A)}{N}\leqslant\mathcal{O}\big((1-\gamma/\gamma_1)^{N/2}\big)\,, \tag{2.22}$$

indicating that the potential between the two types of saddles becomes flatter as the particle number increases.

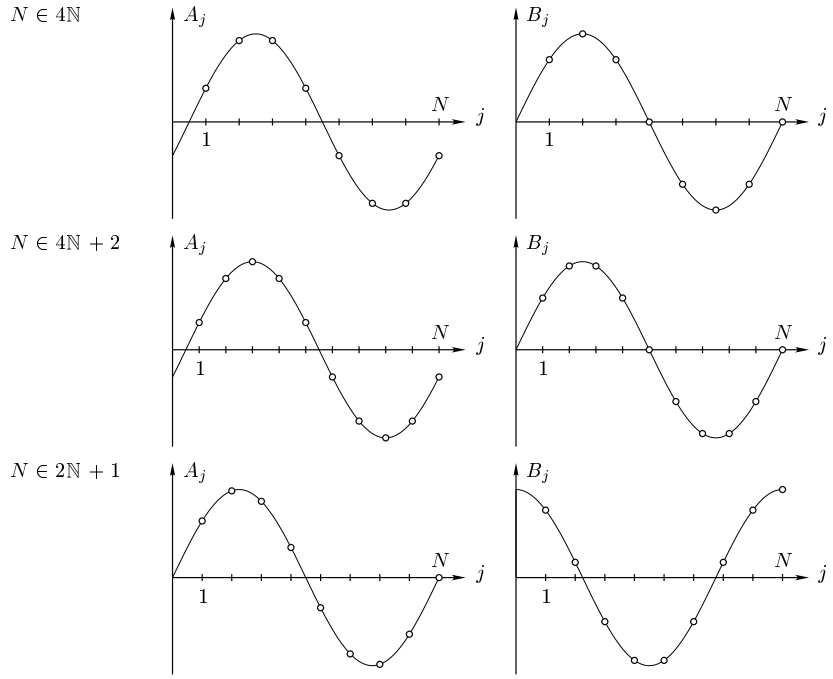

FIGURE 7. Components of the stationary points A and B bifurcating from the origin at $\gamma = \gamma_1$, shown for the three different cases $N = 4L$, $N = 4L+2$ and $N = 2L+1$.

- The components of $A = A(\gamma)$ and $B = B(\gamma)$ are given by

$$A_j(\gamma) = \frac{2}{\sqrt{3}}\sqrt{1-\gamma/\gamma_1}\,\sin\!\left(\frac{2\pi}{N}\big(j-\tfrac{1}{2}\big)\right) + \mathcal{O}\big(1-\gamma/\gamma_1\big)\,,$$
$$B_j(\gamma) = \frac{2}{\sqrt{3}}\sqrt{1-\gamma/\gamma_1}\,\sin\!\left(\frac{2\pi}{N}j\right) + \mathcal{O}\big(1-\gamma/\gamma_1\big)\,, \tag{2.23}$$

  (see Figure 7), except in the case $N = 4$, where

$$A(\gamma) = \sqrt{1-\gamma}\,(1,1,-1,-1) \qquad \text{and} \qquad B(\gamma) = \sqrt{1-\gamma}\,(1,0,-1,0)\,. \tag{2.24}$$

- For any $\gamma \in [0,\gamma_1)$, there exist stationary points $A(\gamma)$ and $B(\gamma)$, satisfying the symmetries indicated in Table 3. The first $N/2$ components of $A(\gamma)$ and the first $N/2-1$ components of $B(\gamma)$ are always positive, and

$$\lim_{\gamma\to 0} A(\gamma) = (1,1,\dots,1,1,-1,-1,\dots,-1,-1)\,,$$
$$\lim_{\gamma\to 0} B(\gamma) = (1,1,\dots,1,0,-1,-1,\dots,-1,0)\,. \tag{2.25}$$

  We do not claim that $A(\gamma)$ and $B(\gamma)$ are continuous in γ everywhere, though we expect them to be so. What we do prove is that for any γ, there is at least one stationary point with the appropriate symmetry (and coordinates of the indicated signs). We also know that A and B depend continuously on γ for γ near 0 and near γ_1. We cannot exclude, however, the presence of saddle–node bifurcations in between.
- We know that the points $A(\gamma)$ are local minima near $\gamma = 0$. Thus these stationary points must undergo at least one secondary bifurcation as γ decreases. For symmetry reasons, we expect that, as in the case $N = 4$ (see Figure 5), there are two successive

symmetry-breaking bifurcations affecting the 1-saddles: First, the mirror symmetry with sign change is broken, then the remaining mirror symmetry is broken as well.
- The error terms in (2.21) and (2.23) may depend on N. The technique we employ here does not allow for an optimal control of the N-dependence of these error terms and of $\delta(N)$. However, in [BFG06b], we obtain such a control in the limit of large N, using different techniques.

Odd particle number

In the case of odd particle number N, the results are slightly weaker, since we are not able to obtain such a precise control on the number of 1-saddles and 2-saddles created in the desynchronisation bifurcation. The main result is the following theorem, which will also be proved in Section 4.3.

Theorem 2.5 (Desynchronisation bifurcation, odd particle number). *Assume that N is odd. Then there exists $\delta = \delta(N) > 0$ such that for $\gamma_1 - \delta < \gamma < \gamma_1$, the set of stationary points $\mathcal{S}(\gamma)$ has cardinality $4\ell N + 3$, for some $\ell \geqslant 1$. All stationary points are saddles of index $0, 1, 2$ or 3, with*

$$\begin{aligned} \mathcal{S}_0 &= O_{I^+} = \{I^+, I^-\} , \\ \mathcal{S}_3 &= O_O = \{O\} , \end{aligned} \tag{2.26}$$

and $|\mathcal{S}_1| = |\mathcal{S}_2| = 2\ell N$. The value $V_\gamma(A)$ of the potential on any saddle A of index 1 satisfies

$$\frac{V_\gamma(A)}{N} = -\frac{1}{6}\big(1 - \gamma/\gamma_1\big)^2 + \mathcal{O}\big((1 - \gamma/\gamma_1)^3\big) . \tag{2.27}$$

In fact, we expect that $\ell = 1$, so that there are exactly $2N$ saddles of index 1 and $2N$ saddles of index 2. This would lead to the following conjecture.

Conjecture 2.6 (Desynchronisation bifurcation, odd particle number). *For odd N and $\gamma_1 - \delta < \gamma < \gamma_1$, the set of stationary points $\mathcal{S}(\gamma)$ has cardinality $4N + 3$. There exist points $A = A(\gamma)$ and $B = B(\gamma)$ in $\mathcal{X}$ such that $\mathcal{S}$ can be decomposed as follows:*

$$\begin{aligned} \mathcal{S}_0 &= O_{I^+} = \{I^+, I^-\} , \\ \mathcal{S}_1 &= O_A = \{A, RA, \dots, R^{N-1}A, -A, -RA, \dots, -R^{N-1}A\} , \\ \mathcal{S}_2 &= O_B = \{B, RB, \dots, R^{N-1}B, -B, -RB, \dots, -R^{N-1}B\} , \\ \mathcal{S}_3 &= O_O = \{O\} . \end{aligned} \tag{2.28}$$

This conjecture would follow as a consequence of a much simpler conjecture on the behaviour of certain coefficients in a centre-manifold expansion, which can be computed iteratively, see Section 4.3. We know that it is true for $N = 3$, and it can be checked by direct computation for the first few values of N. Numerically, we checked the validity of the conjecture for N up to 101. In [BFG06b], we show that the conjecture is also true for sufficiently large N.

Remark 2.7. Again, the proof of the theorem also yields more precise information on the location of the saddles.

- The potential difference between the 2-saddles and 1-saddles satisfies

$$0 < \frac{V_\gamma(B) - V_\gamma(A)}{N} \leqslant \mathcal{O}\big((1 - \gamma/\gamma_1)^N\big) . \tag{2.29}$$

- If the conjecture is true, then the components of $A = A(\gamma)$ and $B = B(\gamma)$ are of the form

$$A_j(\gamma) = \frac{2}{\sqrt{3}}\sqrt{1-\gamma/\gamma_1}\sin\left(\frac{2\pi}{N}j\right) + \mathcal{O}\big(1-\gamma/\gamma_1\big)\ ,$$
$$B_j(\gamma) = \frac{2}{\sqrt{3}}\sqrt{1-\gamma/\gamma_1}\cos\left(\frac{2\pi}{N}j\right) + \mathcal{O}\big(1-\gamma/\gamma_1\big)\ , \tag{2.30}$$

  and satisfy the symmetries indicated in Table 3.
- Independently of the validity of the conjecture, for any $\gamma \in [0, \gamma_1)$, there exist stationary points $A(\gamma)$ and $B(\gamma)$, satisfying the symmetries indicated in Table 3. The first $(N-1)/2$ components of $A(\gamma)$ are strictly positive, and

$$\lim_{\gamma\to 0} A(\gamma) = (1, \dots, 1, -1, \dots, -1, 0)\ . \tag{2.31}$$

2.8 Subsequent Bifurcations

We shall show in Section 3 that the origin undergoes further bifurcations at

$$\gamma = \gamma_M = \frac{1}{1-\cos(2\pi M/N)}\ , \qquad 2 \leqslant M \leqslant \lfloor N/2 \rfloor\ , \tag{2.32}$$

in which the index of the origin O increases by 2 (except for the case where N is even and $M = N/2$, where the index increases by 1), and new saddles $A^{(M)}$ and $B^{(M)}$ of index $2M-1$ and $2M$ are created. Consequently these saddles are not important for the stochastic dynamics, and we shall not provide a detailed analysis here. We briefly mention a few properties of these bifurcations, which we will prove in [BFG06b] to hold for sufficiently large N/M:

- The number of newly created stationary points is given by $4N/\gcd(N, 2M)$, where $\gcd(N, 2M)$ denotes the greatest common divisor of N and $2M$.
- The number of sign changes of x_j as a function of j for these new stationary points is equal to $2M$. M can therefore be considered as a *winding number*.
- If N and M are coprime, the new stationary points x satisfy the symmetries shown in Table 3, while for other M they belong to larger isotropy subgroups.

Example 2.8. For $N = 8$, the origin bifurcates four times as γ decreases from $+\infty$ to 0. We show the symmetries of the bifurcating stationary points in Table 4. They are obtained in the following way:

- Compute the eigenvectors of the Hessian of the potential at the origin;
- Determine the corresponding isotropy subgroups of G_8;
- Write the equation $\dot z = -\nabla V_\gamma(z)$ restricted to the fixed-point set of each isotropy subgroup, and study the bifurcations of the origin in each restricted system.

For instance, for winding number $M = 1$ and orbits of type A, we obtain

$$\begin{aligned} \dot x &= (1-\tfrac{3}{2}\gamma)x + \tfrac{1}{2}\gamma y - x^3\ , \\ \dot y &= \tfrac{1}{2}\gamma x + (1-\tfrac{1}{2}\gamma)y - y^3\ . \end{aligned} \tag{2.33}$$

The origin bifurcates for $\gamma = 2 \pm \sqrt{2}$. An analysis of the linearised system shows that for γ slightly smaller than $2+\sqrt{2}$, the new stationary points must lie in the quadrants

M	γ_M	$\gcd(N, 2M)$	$A^{(M)}$	$B^{(M)}$
1	$2+\sqrt{2}$	2	$(x, y, y, x, -x, -y, -y, -x)$	$(x, y, x, 0, -x, -y, -x, 0)$
2	1	4	$(x, x, -x, -x, x, x, -x, -x)$	$(x, 0, -x, 0, x, 0, -x, 0)$
3	$2-\sqrt{2}$	2	$(x, -y, -y, x, -x, y, y, -x)$	$(x, -y, x, 0, -x, y, -x, 0)$
4	1/2	8	$(x, -x, x, -x, x, -x, x, -x)$	

TABLE 4. Fixed-point sets of the stationary points bifurcating from the origin for $N = 8$, for different winding numbers M. Points of winding number $M = 1$ and $M = 3$ actually have the same fixed point spaces, but we choose the signs of the components in such a way that x and y always have the same sign for the actual stationary points.

$\{(x, y)\colon x > 0, y > 0\}$ and $\{(x, y)\colon x < 0, y < 0\}$. These quadrants, however, are invariant under the flow of $\dot{x} = -\nabla V_\gamma(x)$, since, e.g., $\dot{x} > 0$ if $x = 0$ and $y > 0$, and $\dot{y} > 0$ if $y = 0$ and $x > 0$. Hence the points created in the bifurcation remain in these quadrants. The points created at $\gamma = 2 - \sqrt{2}$, which correspond to the winding number $M = 3$, lie in the complementary quadrants $\{(x, y)\colon x > 0, y < 0\}$ and $\{(x, y)\colon x > 0, y < 0\}$.

For $\gamma = 0$, the only points with the appropriate symmetry are

$$\begin{aligned}
A^{(1)}(0) &= (1, 1, 1, 1, -1, -1, -1, -1)\ , & B^{(1)}(0) &= (1, 1, 1, 0, -1, -1, -1, 0)\ , \\
A^{(2)}(0) &= (1, 1, -1, -1, 1, 1, -1, -1)\ , & B^{(2)}(0) &= (1, 0, -1, 0, 1, 0, -1, 0)\ , \\
A^{(3)}(0) &= (1, -1, -1, 1, -1, 1, 1, -1)\ , & B^{(3)}(0) &= (1, -1, 1, 0, -1, 1, -1, 0)\ , \\
A^{(4)}(0) &= (1, -1, 1, -1, 1, -1, 1, -1)\ . & & \qquad (2.34)
\end{aligned}$$

Note that the cases $M = 2$ and $M = 4$ are obtained by concatenation of multiple copies of stationary points existing for $N = 4$ and $N = 2$, respectively.

2.9 Stochastic Case

We return now to the behaviour of the system of stochastic differential equations

$$\mathrm{d}x_i^\sigma(t) = f(x_i^\sigma(t))\,\mathrm{d}t + \frac{\gamma}{2}\big[x_{i+1}^\sigma(t) - 2x_i^\sigma(t) + x_{i-1}^\sigma(t)\big]\,\mathrm{d}t + \sigma\,\mathrm{d}B_i(t)\ , \qquad i \in \Lambda\ . \quad (2.35)$$

Recall that our main goal is to characterise the noise-induced transition from the configuration $I^- = (-1, -1, \dots, -1)$ to the configuration $I^+ = (1, 1, \dots, 1)$. In particular, we are interested in the time needed for this transition to occur, and in the shape of the critical configuration, i.e., the configuration of highest energy reached in the course of the transition.

Since the probability of a stochastic process in continuous space hitting a given point is typically zero, we have to work with small neighbourhoods of the relevant configurations. Given a Borel set $\mathcal{A} \subset \mathcal{X}$, and an initial condition $x_0 \in \mathcal{X} \setminus \mathcal{A}$, we denote by $\tau^{\mathrm{hit}}(\mathcal{A})$ the *first-hitting time of* $\mathcal{A}$

$$\tau^{\mathrm{hit}}(\mathcal{A}) = \inf\{t > 0\colon x^\sigma(t) \in \mathcal{A}\}\ . \quad (2.36)$$

Similarly, for an initial condition $x_0 \in \mathcal{A}$, we denote by $\tau^{\mathrm{exit}}(\mathcal{A})$ the *first-exit time from* $\mathcal{A}$

$$\tau^{\mathrm{exit}}(\mathcal{A}) = \inf\{t > 0\colon x^\sigma(t) \notin \mathcal{A}\}\ . \quad (2.37)$$

We can now formulate our main results, which are similar in spirit to Theorems 3.2.1 and 4.2.1 of [dH04].

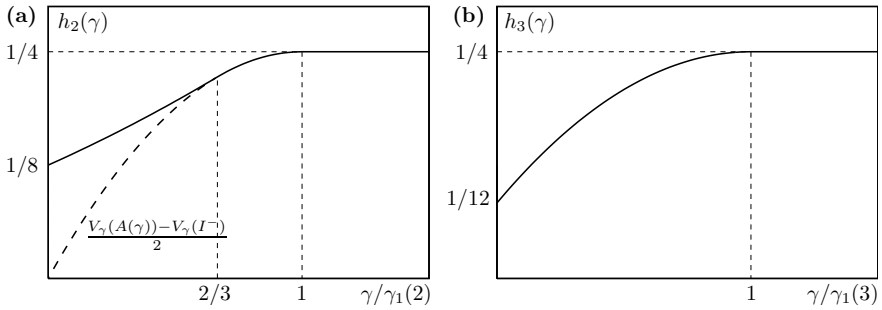

FIGURE 8. The normalised potential differences $h_N(\gamma)$ for $N = 2$ and $N = 3$. The broken curve for $N = 2$ shows the potential difference $(V_\gamma(A) - V_\gamma(I^-))/2$, which is smaller than $h_N(\gamma)$ for $\gamma/\gamma_1 < 2/3$ (compare (2.18)), because for these parameter values, the 1-saddle is the point labelled *Aa*. For general particle number N, we know that $h_N(\gamma)$ behaves like $1/4 - c_N(1 - \gamma/\gamma_1)^2$ as $\gamma \nearrow \gamma_1$, and that $h_N(0) = 1/4N$.

Theorem 2.9 (Stochastic case, synchronisation regime). *Assume that the coupling strength satisfies $\gamma > \gamma_1 = (1 - \cos(2\pi/N))^{-1}$. We fix radii $0 < r < R < 1/2$, and denote by $\tau_+ = \tau^{\mathrm{hit}}(\mathcal{B}(I_+, r))$ the first-hitting time of a ball $\mathcal{B}(I^+, r)$ of radius r around I^+. Then for any initial condition $x_0 \in \mathcal{B}(I^-, r)$, any $N \geqslant 2$ and any $\delta > 0$,*

$$\lim_{\sigma\to 0} \mathbb{P}^{x_0}\bigl\{ \mathrm{e}^{(N/2-\delta)/\sigma^2} < \tau_+ < \mathrm{e}^{(N/2+\delta)/\sigma^2} \bigr\} = 1 \tag{2.38}$$

and

$$\lim_{\sigma\to 0} \sigma^2 \log \mathbb{E}^{x_0}\left\{\tau_+\right\} = \frac{N}{2} \, . \tag{2.39}$$

Furthermore, let $\tau_O = \tau^{\mathrm{hit}}(\mathcal{B}(O, r))$, and let

$$\tau_- = \inf\{t > \tau^{\mathrm{exit}}(\mathcal{B}(I^-, R))\colon x_t \in \mathcal{B}(I^-, r)\} \tag{2.40}$$

be the time of first return to the small ball $\mathcal{B}(I^-, r)$ around I^- after leaving the larger ball $\mathcal{B}(I^-, R)$. Then

$$\lim_{\sigma\to 0} \mathbb{P}^{x_0}\bigl\{ \tau_O < \tau_+ \bigm| \tau_+ < \tau_- \bigr\} = 1 \, . \tag{2.41}$$

We will omit the proof of this result, which is a direct consequence of Proposition 2.2 and standard results in Wentzell–Freidlin theory, see for instance [FW98, Sug96, Kif81].

Relations (2.38) and (2.39) mean that the transition from I^- to I^+ typically takes a time of order $\mathrm{e}^{N/2\sigma^2}$. Relation (2.41) shows that, provided a transition from $\mathcal{B}(I^-, r)$ to $\mathcal{B}(I^+, r)$ is observed, the process is likely to pass close to the saddle at the origin on its way from one potential well to the other one. The origin thus plays the rôle of the critical configuration in the synchronisation regime.

Theorem 2.10 (Stochastic case, desynchronised regime). *Assume $\gamma < \gamma_1$. Let r, R and τ_+ and τ_- be defined as in Theorem 2.9, and fix an initial condition $x_0 \in \mathcal{B}(I^-, r)$. Let $h_N(\gamma) = (V_\gamma(A) - V_\gamma(I^-))/N$ denote the normalised potential difference between 1-saddles and potential minima at I^-. Then $h_N(\gamma)$ satisfies*

$$h_N(\gamma) = \frac{1}{4} - c_N\bigl(1 - \gamma/\gamma_1\bigr)^2 + \mathcal{O}\bigl((1 - \gamma/\gamma_1)^3\bigr) \qquad \text{as } \gamma \nearrow \gamma_1 \, , \tag{2.42}$$

where $c_2 = c_4 = 1/4$ and $c_N = 1/6$ for $N = 3$ and all $N \geqslant 5$, and one has

$$\lim_{\sigma\to 0} \mathbb{P}^{x_0}\bigl\{ \mathrm{e}^{(2Nh_N(\gamma)-\delta)/\sigma^2} < \tau_+ < \mathrm{e}^{(2Nh_N(\gamma)+\delta)/\sigma^2} \bigr\} = 1 \, , \tag{2.43}$$

and

$$\lim_{\sigma\to 0} \sigma^2 \log \mathbb{E}^{x_0}\{\tau_+\} = 2Nh_N(\gamma)\ . \tag{2.44}$$

Furthermore, assume that either N is even, or N is odd and Conjecture 2.6 holds. Let

$$\tau_A = \tau^{\mathrm{hit}}\Big(\bigcup_{g\in G} \mathcal{B}(gA(\gamma), r)\Big)\ . \tag{2.45}$$

Then there exists a $\delta = \delta(N) > 0$ such that for $\gamma_1 - \delta < \gamma < \gamma_1$

$$\lim_{\sigma\to 0} \mathbb{P}^{x_0}\big\{\tau_A < \tau_+ \,\big|\, \tau_+ < \tau_-\big\} = 1\ . \tag{2.46}$$

The proof is again standard, and we will omit it here.

Relations (2.43) and (2.44) mean that the transition from I^- to I^+ typically takes a time of order $\mathrm{e}^{2Nh_N(\gamma)/\sigma^2}$, while relation (2.46) shows that the set of critical configurations is the orbit of $A(\gamma)$.

We conclude the statement of results with a few comments:

- The very precise results in [BEGK04, BGK05] allow in principle for a more precise control of the expected transition time τ_+ than the exponential asymptotics given in (2.39) and (2.44). However, these results cannot be applied directly to our case, because they assume some non-degeneracy condition to hold for the potential, which excludes symmetries as in the system we are investigating. Therefore, in the present work we content ourselves with the exponential asymptotics. A finer analysis is feasible, and we plan to provide such a further study.
- We have seen that the potential difference between the 1-saddles A and the 2-saddles B becomes smaller and smaller as the particle number increases. As a consequence, for any given noise intensity $\sigma > 0$, the transition paths become less localised as the particle number N increases. This reflects the fact that the system becomes translation-invariant in the large-N limit.
- As the coupling intensity γ decreases, the configurations of highest energy reached in the course of a transition become more and more inhomogeneous along the chain, and we expect them to converge to configurations of the form $(1, \dots, 1, 0, -1, \dots, -1)$ in the uncoupled limit. In addition, several local minima and saddles should appear by saddle–node bifurcations along the optimal transition path, thereby increasing the number of metastable states of the system.

3 Lyapunov Functions and Synchronisation

We now turn to the proofs of the statements made in Section 2, and start by introducing a few notations. The "interaction part" of the potential is proportional to

$$W(x) = \frac{1}{2}\sum_{i\in\Lambda}(x_i - x_{i+1})^2 = \frac{1}{2}\|x - Rx\|^2 = \langle x, \Sigma x\rangle \;, \tag{3.1}$$

where Σ is the symmetric matrix $\Sigma = \mathbb{1} - \frac{1}{2}(R + R^{\mathrm{T}})$. Hence, the potential $V_\gamma(x)$ can be written as

$$V_\gamma(x) = -\frac{1}{2}\langle x, (\mathbb{1} - \gamma\Sigma)x\rangle + \frac{1}{4}\sum_{i\in\Lambda} x_i^4 \;. \tag{3.2}$$

The eigenvectors of Σ are of the form $v_k = (1, \omega^k, \dots, \omega^{(N-1)k})^{\mathrm{T}}$, $k = 0, \dots, N-1$, where $\omega = \mathrm{e}^{2\pi\,\mathrm{i}/N}$, with eigenvalues $1 - \cos(2\pi k/N)$. This implies in particular that the Hessian of the potential at the origin, which is given by $\gamma\Sigma - \mathbb{1}$, has eigenvalues $-\lambda_k$, where

$$\lambda_k = \lambda_{-k} = 1 - \gamma\left(1 - \cos\frac{2\pi k}{N}\right) = 1 - \frac{\gamma}{\gamma_k} \;. \tag{3.3}$$

The origin is a 1-saddle for $\gamma > \gamma_1$. As γ decreases, the index of the origin increases by 2 each time γ crosses one of the γ_k, until it becomes an N-saddle at $\gamma = \gamma_{\lfloor N/2\rfloor}$.

We now show that for $\gamma > \gamma_1$ (i.e., $\lambda_1 < 0$), $W(x)$ is a Lyapunov function for the deterministic system $\dot{x} = -\nabla V_\gamma(x)$.

Proposition 3.1. *For any initial condition x_0, the solution $x(t)$ of $\dot{x} = -\nabla V_\gamma(x)$ satisfies*

$$\frac{\mathrm{d}}{\mathrm{d}t}W(x(t)) \leqslant 2\big(1 - \gamma/\gamma_1\big)W(x(t)) - \frac{1}{N}W(x(t))^2 \;. \tag{3.4}$$

As a consequence, if γ is strictly larger than γ_1, then $x(t)$ converges exponentially fast to the diagonal, and thus the only equilibrium points of the system are O and $I^{\pm}$.

Proof: We first observe that the relation

$$f(x_i) - f(x_{i+1}) = (x_i - x_{i+1})\big[1 - (x_i^2 + x_i x_{i+1} + x_{i+1}^2)\big] \tag{3.5}$$

allows us to write

$$\frac{\mathrm{d}}{\mathrm{d}t}(x - Rx) = \Pi(x,\gamma)(x - Rx) \;, \tag{3.6}$$

where $\Pi(x,\gamma) = \mathbb{1} - \gamma\Sigma - D(x)$. Here $D(x)$ is a diagonal matrix, whose ith entry is given by $x_i^2 + x_i x_{i+1} + x_{i+1}^2$, and can be bounded below by $\frac{1}{4}(x_i - x_{i+1})^2$. It follows

$$\begin{aligned}
\frac{\mathrm{d}}{\mathrm{d}t}W(x(t)) &= \langle x - Rx, \frac{\mathrm{d}}{\mathrm{d}t}(x - Rx)\rangle \\
&= \langle x - Rx, \Pi(x,\gamma)(x - Rx)\rangle \\
&\leqslant \langle x - Rx, (\mathbb{1} - \gamma\Sigma)(x - Rx)\rangle - \frac{1}{4}\sum_{i\in\Lambda}(x_i - x_{i+1})^4 \\
&\leqslant \lambda_1\|x - Rx\|^2 - \frac{1}{4N}\|x - Rx\|^4
\end{aligned} \tag{3.7}$$

by Cauchy-Schwartz. This implies (3.4). If $\gamma \geqslant \gamma_1$, then $W(x(t))$ converges to zero as $t \to \infty$ for all initial conditions, which implies that all stationary points $x^\star$ must satisfy $W(x^\star) = 0$, and thus lie on the diagonal. The only stationary points on the diagonal, however, are O and $I^{\pm}$. □

PROOF OF PROPOSITION 2.2. The assertion on the unstable manifold follows from the invariance of the diagonal and the fact that O is a 1-saddle if and only if $\gamma > \gamma_1$. For $\gamma < \gamma_1$, we will show independently that there exist stationary points outside the diagonal. Note however that relation (3.4) shows that these points must lie in a small neighbourhood of the diagonal for γ sufficiently close to γ_1. □

Let us also point out that the growth of the potential away from the diagonal can be controlled in the following way.

Proposition 3.2. *For any $x_\parallel \in \mathcal{D}$ and $x_\perp$ orthogonal to the diagonal $\mathcal{D}$, the potential satisfies*

$$V_\gamma(x_\parallel + x_\perp) \geqslant V_\gamma(x_\parallel) + \frac{1}{2}\Big(\frac{\gamma}{\gamma_1} - 1\Big)\|x_\perp\|^2 \,. \tag{3.8}$$

PROOF: Using (3.2) and the fact that $\Sigma x_\parallel = 0$, we obtain for any $\lambda \in \mathbb{R}$

$$V_\gamma(x_\parallel + \lambda x_\perp) = -\frac{1}{2}(\|x_\parallel\|^2 + \lambda^2\|x_\perp\|^2) + \frac{1}{4}\sum_{i=1}^{N}([x_\parallel + \lambda x_\perp]_i)^4 + \frac{\gamma}{2}\lambda^2\langle x_\perp, \Sigma x_\perp\rangle \,. \tag{3.9}$$

The scalar product $\langle x_\perp, \Sigma x_\perp\rangle$ can be bounded below by $\|x_\perp\|^2/\gamma_1$. Moreover, applying Taylor's formula to second order in λ, and using the fact that all components of $x_\parallel$ are equal while the sum of the components of $x_\perp$ vanishes, (3.8) follows. □

4 Fourier Representation

Let $\omega = \mathrm{e}^{2\pi\,\mathrm{i}\,/N}$. The Fourier variables are defined by the linear transformation

$$y_k = \frac{1}{N}\sum_{j\in\Lambda}\overline{\omega}^{jk}x_j \,, \qquad\qquad k \in \Lambda^* = \mathbb{Z}\,/N\mathbb{Z} \,. \tag{4.1}$$

The inverse transformation is given by

$$x_j = \sum_{k\in\Lambda^*}\omega^{jk}y_k \,, \tag{4.2}$$

as a consequence of the fact that $\sum_{j=1}^{N}\omega^{j(k-\ell)} = N\delta_{k\ell}$. Note that $y_k = \overline{y_{-k}}$, so that we might use the real and imaginary parts of y_k as dynamical variables, instead of y_k and y_{-k}. The following result is obtained by a direct computation.

Proposition 4.1. *In Fourier variables, the equation of motion $\dot{x} = -\nabla V_\gamma(x)$ takes the form*

$$\dot{y}_k = \lambda_k y_k - \sum_{\substack{k_1,k_2,k_3\in\Lambda^*\\ k_1+k_2+k_3=k}} y_{k_1}y_{k_2}y_{k_3} \,, \tag{4.3}$$

where the λ_k are those defined in (3.3)*. Furthermore, the potential is given in terms of Fourier variables by*

$$\widehat{V}_\gamma(y) = -\frac{N}{2}\sum_{k\in\Lambda^*}\lambda_k|y_k|^2 + \frac{N}{4}\sum_{\substack{k_1,k_2,k_3,k_4\in\Lambda^*\\ k_1+k_2+k_3+k_4=0}} y_{k_1}y_{k_2}y_{k_3}y_{k_4} \,. \tag{4.4}$$

R	$x_j \mapsto x_{j+1}$	$y_k \mapsto \omega^k y_k$
$RS = SR^{-1}$	$x_j \mapsto x_{N-j}$	$y_k \mapsto \overline{y_k} = y_{-k}$
C	$x_j \mapsto -x_j$	$y_k \mapsto -y_k$

TABLE 5. Effect of a set of generators of the symmetry group G_N on Fourier variables.

The effect of the symmetries on the Fourier variables is fully determined by the action of three generators of the symmetry group G, as shown in Table 5.

A particular advantage of the Fourier representation is that certain invariant sets of phase space take a simple form in these variables. For instance, for any ℓ,

$$x_{\ell-j} = x_j \ \forall j \qquad \Rightarrow \qquad \overline{\omega}^{\ell k}\overline{y_k} = y_k \ \forall k \qquad \Rightarrow \qquad y_k = \omega^{\ell k/2} r_k \ \forall k \tag{4.5}$$

where the r_k are all real. Similarly, for any ℓ,

$$x_{\ell-j} = -x_j \ \forall j \qquad \Rightarrow \qquad \overline{\omega}^{\ell k}\overline{y_k} = -y_k \ \forall k \qquad \Rightarrow \qquad y_k = \mathrm{i}\,\omega^{\ell k/2} r_k \ \forall k \tag{4.6}$$

where the r_k are all real.

4.1 The Case $N = 2$

For $N = 2$, we have $\omega = -1$, and the Fourier variables are simply $y_0 = (x_1 + x_2)/2$, $y_1 = (x_2 - x_1)/2$. The equations (4.3) become

$$\begin{aligned} \dot{y}_0 &= y_0\big[1 - (y_0^2 + 3y_1^2)\big] \ , \\ \dot{y}_1 &= y_1\big[\lambda_1 - (3y_0^2 + y_1^2)\big] \ , \end{aligned} \tag{4.7}$$

with $\lambda_1 = 1 - 2\gamma$. The potential is given by

$$\widehat{V}_\gamma(y) = -y_0^2 - \lambda_1 y_1^2 + \frac{1}{2}(y_0^4 + 6y_0^2 y_1^2 + y_1^4) \ . \tag{4.8}$$

Proposition 4.2. *The bifurcation diagram for $N = 2$ is the one given in Figure 3, and the value of the potential on the bifurcating branches is given by*

$$V_\gamma(A) = -\frac{1}{2}\lambda_1^2 \ , \qquad V_\gamma(Aa) = \frac{1}{16}(\lambda_1^2 - 6\lambda_1 + 1) \ . \tag{4.9}$$

PROOF: In addition to the origin, there can be three types of stationary points:

- If $y_1 = 0$, $y_0 \neq 0$, then necessarily $y_0 = \pm 1$, yielding the stationary points $I^\pm$ in original variables.
- If $y_0 = 0$, $y_1 \neq 0$, there are two additional points A, RA, given by $y_1 = \pm\sqrt{\lambda_1}$ whenever $\lambda_1 > 0$, i.e., $\gamma < 1/2$. In original variables, these have the expression $(\pm\sqrt{\lambda_1}, \mp\sqrt{\lambda_1})$, so that they have the $(x, -x)$-symmetry.
- If $y_0, y_1 \neq 0$, there are four additional points, given by $8y_0^2 = 3\lambda_1 - 1$, $8y_1^2 = 3 - \lambda_1$, provided $\lambda_1 > 1/3$, i.e., $\gamma < 1/3$.

It is straightforward to check the stability of these stationary points from the Jacobian matrix of (4.7), and to compute the value of the potential, using (4.8). □

4.2 The Case $N = 3$

For $N = 3$, we choose $\Lambda^* = \{-1, 0, 1\}$. The equations in Fourier variables read

$$\begin{aligned} \dot{y}_0 &= y_0 - (y_0^3 + y_1^3 + \overline{y_1}^3 + 6y_0|y_1|^2) \;, \\ \dot{y}_1 &= \lambda_1 y_1 - 3(y_1|y_1|^2 + y_0\overline{y_1}^2 + y_0^2 y_1) \;, \end{aligned} \tag{4.10}$$

with $\lambda_1 = 1 - \frac{3}{2}\gamma$.

Proposition 4.3. *The bifurcation diagram for $N = 3$ is the one given in Figure 4, where the saddle–node bifurcations occur for*

$$\gamma = \gamma^\star(3) = \frac{\sqrt{3 + 2\sqrt{3}} - \sqrt{3}}{3} \simeq 0.2701\ldots \;. \tag{4.11}$$

On the 1-saddles, the potential has value

$$V_\gamma(A) = -\frac{1}{2}\lambda_1^2 \;. \tag{4.12}$$

Proof: Using polar coordinates $y_1 = r_1\,\mathrm{e}^{\mathrm{i}\,\varphi_1}$, the equations (4.10) become

$$\begin{aligned} \dot{y}_0 &= y_0(1 - y_0^2 - 6r_1^2) - 2r_1^3\cos 3\varphi_1 \;, \\ \dot{r}_1 &= r_1\big[\lambda_1 - 3(r_1^2 + y_0 r_1\cos 3\varphi_1 + y_0^2)\big] \;, \\ \dot{\varphi}_1 &= 3y_0 r_1 \sin 3\varphi_1 \;. \end{aligned} \tag{4.13}$$

In addition to the origin, there can be three types of stationary points:

- If $r_1 = 0$, $y_0 \neq 0$, then necessarily $y_0 = \pm 1$, yielding the points $I^\pm$.
- If $y_0 = 0$, $r_1 \neq 0$, we obtain six stationary points given by $r_1 = \sqrt{\lambda_1/3}$ and $\cos 3\varphi_1 = 0$, provided $\lambda_1 > 0$, that is, $\gamma < 2/3$. These points have one of the symmetries $(x, -x, 0)$, $(x, 0, -x)$ or $(0, x, -x)$.
- If $\sin 3\varphi_1 = 0$, it is sufficient by symmetry to consider the case $\varphi_1 = 0$ (i.e., y_1 real). These points have the (x, x, y)-symmetry. Setting $y_0 = u + v$, $r_1 = u - v$, we find that stationary points should satisfy the relations

$$\begin{aligned} \lambda_1/3 &= 3u^2 + v^2 \;, \\ 0 &= 24u^2 v + (1 - \lambda_1)u + (1 - \tfrac{5}{3}\lambda_1)v \;. \end{aligned} \tag{4.14}$$

  Taking the square of the second equation and eliminating u yields a cubic equation for v^2. In fact, the variable $z = v^2 - (1 + \lambda_1)/12$ satisfies

$$z^3 - \lambda z + \mu = 0 \;, \qquad \lambda = \frac{\lambda_1}{48} \;, \qquad \mu = \frac{1 - 3\lambda_1 + 6\lambda_1^2 - 2\lambda_1^3}{1728} \;. \tag{4.15}$$

  This equation has three roots for λ_1 slightly smaller than 1, and one root for $\lambda_1 = 0$. Bifurcations occur whenever the condition $27\mu^2 = 4\lambda^3$ is fulfilled, which turns out to be equivalent to $(1 - \lambda_1)^2 g(\lambda_1) = 0$, where

$$g(\lambda_1) = 4\lambda_1^4 - 16\lambda_1^3 + 12\lambda_1^2 - 4\lambda_1 + 1 \;. \tag{4.16}$$

  Since $g(0) = 1$ and $g(1) = -3$, and it is easy to check that $g' < 0$ on $[0, 1]$, there can be only one bifurcation point in this interval, whose explicit value leads to the bifurcation value (4.11). □

4.3 Centre-Manifold Analysis of the Desynchronisation Bifurcation

Assume $N \geqslant 3$. We consider now the behaviour for γ close to γ_1, i.e., for λ_1 close to 0. Setting $z = (y_0, y_2, y_{-2}, \dots)$, the equation (4.3) in Fourier variables is of the form

$$\dot{y}_k = \lambda_k y_k + g_k(y_1, \overline{y_1}, z) \;, \tag{4.17}$$

where

$$g_k(y_1, \overline{y_1}, z) = - \sum_{\substack{k_1,k_2,k_3 \in \Lambda^* \\ k_1+k_2+k_3=k}} y_{k_1} y_{k_2} y_{k_3} \;. \tag{4.18}$$

For small λ_1, the system admits an invariant centre manifold of equation

$$y_k = h_k(y_1, \overline{y_1}, \lambda_1) \;, \qquad k \neq \pm 1 \;, \tag{4.19}$$

where the h_k satisfy the partial differential equations

$$\lambda_k h_k + g_k(y_1, \overline{y_1}, \{h_j\}_j) = \frac{\partial h_k}{\partial y_1}\big[\lambda_1 y_1 + g_1(y_1, \overline{y_1}, \{h_j\}_j)\big] + \frac{\partial h_k}{\partial \overline{y_1}}\overline{\big[\lambda_1 y_1 + g_1(y_1, \overline{y_1}, \{h_j\}_j)\big]} \;. \tag{4.20}$$

We fix a cut-off order K. For our purposes, $K = 2N$ will be sufficient. We are looking for an expansion of the form

$$h_k(y_1, \overline{y_1}, \lambda_1) = \sum_{\substack{n,m \geqslant 0 \\ 3 \leqslant n+m < K}} h^k_{nm}(\lambda_1) {y_1}^n \overline{y_1}^m + \mathcal{O}(|y_1|^K) \;. \tag{4.21}$$

First it is useful to examine the effect of symmetries on the coefficients.

Lemma 4.4. *The coefficients in the expansion of the centre manifold satisfy*

- $h^k_{nm}(\lambda_1) \in \mathbb{R}$ *;*
- $h^k_{nm}(\lambda_1) = h^{-k}_{mn}(\lambda_1)$*;*
- $h^k_{nm}(\lambda_1) = 0$ *if* $n - m \neq k \pmod N$*;*
- $h^k_{nm}(\lambda_1) = 0$ *if* $n + m$ *is even.*

Proof: The centre manifold has the same symmetries as the equations (4.3). Thus

- The R-symmetry requires $\omega^k h_k(y_1, \overline{y_1}, \lambda_1) = h_k(\omega y_1, \overline{\omega y_1}, \lambda_1)$, yielding the condition $(\omega^k - \omega^{n-m}) h^k_{nm}(\lambda_1) = 0$ so that $h^k_{nm}(\lambda_1)$ vanishes unless $n - m = k \pmod N$;
- The RS-symmetry requires $\overline{h_k(y_1, \overline{y_1}, \lambda_1)} = h_k(\overline{y_1}, y_1, \lambda_1)$, and yields the reality of the coefficients;
- The C-symmetry requires $-h_k(y_1, \overline{y_1}, \lambda_1) = h_k(-y_1, -\overline{y_1}, \lambda_1)$, yielding the condition $((-1)^{n+m} + 1) h^k_{nm}(\lambda_1) = 0$, so that $h^k_{nm}(\lambda_1)$ vanishes unless $n + m$ is odd;
- The condition $h_{-k}(y_1, \overline{y_1}, \lambda_1) = \overline{h_k(y_1, \overline{y_1}, \lambda_1)}$ yields the symmetry under permutation of n and m. □

From now on, we will write $n - m \equiv k$ instead of $n - m = k \pmod N$. Lemma 4.4 allows us to simplify the notation, setting

$$h_k(y_1, \overline{y_1}, \lambda_1) = \sum_{\substack{n,m \geqslant 0,\ 3 \leqslant n+m < K \\ n-m \equiv k}} h_{nm}(\lambda_1) {y_1}^n \overline{y_1}^m + \mathcal{O}(|y_1|^K) \;. \tag{4.22}$$

It is convenient to set $h_1(y_1, \overline{y_1}, \lambda_1) = y_1$ and $h_{-1}(y_1, \overline{y_1}, \lambda_1) = \overline{y_1}$. Then (4.22) holds for $k = \pm 1$ as well if we set $h_{nm} = \delta_{n1}\delta_{m0}$ whenever $n - m \equiv 1$, and $h_{nm} = \delta_{n0}\delta_{m1}$ whenever $n - m \equiv -1$. The equation on the centre manifold can be written as

$$\begin{aligned}\dot{y}_1 &= \lambda_1 y_1 - \sum_{k_1+k_2+k_3=1} h_{k_1}(y_1, \overline{y_1}, \lambda_1) h_{k_2}(y_1, \overline{y_1}, \lambda_1) h_{k_3}(y_1, \overline{y_1}, \lambda_1) \\ &= \lambda_1 y_1 - \sum_{\substack{n,m\geqslant 0,\ 3\leqslant n+m<K \\ n-m\equiv 1}} c_{nm}(\lambda_1) y_1^n \overline{y_1}^m + \mathcal{O}(|y_1|^K) \,, \end{aligned} \tag{4.23}$$

where

$$c_{nm}(\lambda_1) = \sum_{\substack{n_i\geqslant 0\colon\ n_1+n_2+n_3=n \\ m_i\geqslant 0\colon\ m_1+m_2+m_3=m}} h_{n_1m_1}(\lambda_1) h_{n_2m_2}(\lambda_1) h_{n_3m_3}(\lambda_1) \in \mathbb{R} \,. \tag{4.24}$$

Note that $c_{nm}(\lambda_1) = 0$ whenever $n + m$ is even. In polar coordinates $y_1 = r_1 \, \mathrm{e}^{\mathrm{i}\,\varphi_1}$, Equation (4.23) becomes

$$\begin{aligned}\dot{r}_1 &= \lambda_1 r_1 - \sum_{\substack{n,m\geqslant 0,\ 3\leqslant n+m<K \\ n-m\equiv 1}} c_{nm}(\lambda_1) r_1^{n+m} \cos\bigl((n-m-1)\varphi_1\bigr) + \mathcal{O}(r_1^K) \,, \\ \dot{\varphi}_1 &= - \sum_{\substack{n,m\geqslant 0,\ 3\leqslant n+m<K \\ n-m\equiv 1}} c_{nm}(\lambda_1) r_1^{n+m-1} \sin\bigl((n-m-1)\varphi_1\bigr) + \mathcal{O}(r_1^{K-1}) \,. \end{aligned} \tag{4.25}$$

In general, $c_{21} = 3h_{10}^2 h_{01} = 3$ is the only term contributing to the third-order term of $\dot{r}_1$. The only exception is the case $N = 4$, in which $c_{03} = h_{10}^3 = 1$ also contributes to the lowest order, yielding

$$\dot{r}_1 = \begin{cases} \lambda_1 r_1 - 3r_1^3 + \mathcal{O}(r_1^5) & \text{if } N \neq 4 \,, \\ \lambda_1 r_1 - (3 + \cos 4\varphi_1) r_1^3 + \mathcal{O}(r_1^5) & \text{if } N = 4 \,. \end{cases} \tag{4.26}$$

This shows that all stationary points bifurcating from the origin lie at a distance of order $\sqrt{\lambda_1}$ from it: They satisfy $r_1 = \sqrt{\lambda_1/(3 + \cos 4\varphi_1)} + \mathcal{O}(\lambda_1^{3/2})$ in the case $N = 4$, and $r_1 = \sqrt{\lambda_1/3} + \mathcal{O}(\lambda_1^{3/2})$ otherwise.

The terms with $n - m = 1$ do not contribute to the angular derivative $\dot{\varphi}_1$. In the particular case $N = 4$, we have

$$\dot{\varphi}_1 = \sin(4\varphi_1) r_1^2 + \mathcal{O}(r_1^4) \,, \tag{4.27}$$

yielding 8 stationary points, of alternating stability. Otherwise, we have to distinguish between two cases:

- If N is even, the lowest-order coefficient contributing to $\dot{\varphi}_1$ is $c_{0,N-1}$, giving

  $$\dot{\varphi}_1 = c_{0,N-1}(\lambda_1) r_1^{N-2} \sin(N\varphi_1) + \mathcal{O}(r_1^{N-1}) \,. \tag{4.28}$$

  Thus if we prove that $c_{0,N-1}(\lambda_1) \neq 0$, we will have obtained the existence of exactly $2N$ stationary points, of alternating stability, bifurcating from the origin.

- If N is odd, then $n+m$ is even whenever $n-m = \pm N+1$, which implies by Lemma 4.4 that $c_{nm} = 0$ for these (n,m). The lowest-order coefficient contributing to $\dot\varphi_1$ is thus $c_{0,2N-1}$, giving

$$\dot\varphi_1 = c_{0,2N-1}(\lambda_1) r_1^{2N-2} \sin(2N\varphi_1) + \mathcal{O}(r_1^{2N-1}) \; . \tag{4.29}$$

  Thus if we prove that $c_{0,2N-1}(\lambda_1) \neq 0$, we will have obtained the existence of exactly $4N$ stationary points, of alternating stability, bifurcating from the origin.

Remark 4.5. Let r_1 and r_1' be solutions of the equation $\dot r_1 = 0$ obtained for two different values of φ_1, say $\varphi_1 = 0$ and $\varphi_1 = \pi/N$. For even N, using the fact that the terms up to order $N-2$ in the first equation in (4.25) do not depend on φ_1, one can see that $r_1' - r_1 = \mathcal{O}(\lambda_1^{(N-3)/2})$. For odd N, one obtains in a similar way $r_1' - r_1 = \mathcal{O}(\lambda_1^{(2N-3)/2})$.

In order to compute sign of the coefficients $c_{0,N-1}$ or $c_{0,2N-1}$, we need at least to know the coefficients h_{0m} for odd m up to $N-3$ or $2N-3$, respectively. By continuity, however, it is sufficient to compute them for $\lambda_1 = 0$. We henceforth set $h_{nm} = h_{nm}(0)$.

Lemma 4.6. *For all odd $m > 0$ such that $m \not\equiv \pm 1$, $h_{0m} = h_{m0}$ satisfies*

$$\begin{aligned}
\lambda_m h_{0m} = & \sum_{m_i \geqslant 0 \colon m_1+m_2+m_3=m} h_{0m_1} h_{0m_2} h_{0m_3} \\
& - \sum_{\substack{v \geqslant 0 \colon v \equiv m+1 \\ m_i \geqslant 0 \colon m_1+m_2+m_3+v=m}} h_{0m_1} h_{0m_2} h_{0m_3} h_{1v} \\
& - \sum_{\substack{v > 0 \colon v \equiv m \\ n_i \geqslant 0 \colon n_1+n_2+n_3+v=m+1}} v h_{n_1 0} h_{n_2 0} h_{n_3 0} h_{0v} \; .
\end{aligned} \tag{4.30}$$

Furthermore, if either N is even and $1 \leqslant m \leqslant N-3$, or N is odd and $1 \leqslant m \leqslant 2N-3$, then

$$\lambda_m h_{0m} = \sum_{m_i \geqslant 0 \colon m_1+m_2+m_3=m} h_{0m_1} h_{0m_2} h_{0m_3} \; . \tag{4.31}$$

Proof: By invariance of the centre manifold, $h_k(y_1, \overline{y_1}, 0)$ has to satisfy the equation

$$\lambda_k h_k = -g_k(y_1, \overline{y_1}, \{h_j\}_j) + \frac{\partial h_k}{\partial y_1} g_1(y_1, \overline{y_1}, \{h_j\}_j) + \frac{\partial h_k}{\partial \overline{y_1}} \overline{g_1(y_1, \overline{y_1}, \{h_j\}_j)} \; . \tag{4.32}$$

Plugging in the series (4.18) of g_k and (4.22) of h_k, this can be seen to be equivalent to

$$\begin{aligned}
\lambda_{n-m} h_{nm} = & \sum_{\substack{n_i \geqslant 0 \colon n_1+n_2+n_3=n \\ m_i \geqslant 0 \colon m_1+m_2+m_3=m}} h_{n_1 m_1} h_{n_2 m_2} h_{n_3 m_3} \\
& - \sum_{\substack{u,v \geqslant 0 \colon u-v \equiv n-m \\ n_i \geqslant 0 \colon n_1+n_2+n_3+u=n+1 \\ m_i \geqslant 0 \colon m_1+m_2+m_3+v=m}} u h_{n_1 m_1} h_{n_2 m_2} h_{n_3 m_3} h_{uv} \\
& - \sum_{\substack{u,v \geqslant 0 \colon u-v \equiv n-m \\ n_i \geqslant 0 \colon n_1+n_2+n_3+v=m+1 \\ m_i \geqslant 0 \colon m_1+m_2+m_3+u=n}} v h_{n_1 m_1} h_{n_2 m_2} h_{n_3 m_3} h_{uv} \; .
\end{aligned} \tag{4.33}$$

In the special case $n = 0$, the second sum vanishes unless $u = 1$, and $n_1 = n_2 = n_3 = 0$. In the third sum, we must have $v > 0$ and $u = m_1 = m_2 = m_3 = 0$. Finally, the fact that $\lambda_{-m} = \lambda_m$ yields (4.30).

Assume now that N is even and $m \leqslant N - 3$. In the second sum, v cannot exceed m, but then the condition $v \equiv m + 1$ would require $m \geqslant N - 1$. Thus the second sum vanishes. In the third sum, v cannot exceed $m + 1$, and thus $v = m$. However, in that case $n_1 + n_2 + n_3 = 1$, so that two n_i must be zero. Since $h_{00} = 0$, the third sum vanishes as well.

If N is odd and $m \leqslant 2N - 3$, then the second sum in (4.30) allows for $v = m + 1 - N$. Then, however, we would have $m_1 + m_2 + m_3 = N - 1$, which is even. Thus at least one of the m_i is even, yielding a vanishing summand. The third sum in (4.30) allows for $v = m$ and $v = m - N$. In the first case, however, the summand vanishes for the same reason as before, while in the second case, we would have $n_1 + n_2 + n_3 = N + 1$, which is even. Thus at least one of the n_i is even, yielding again a vanishing summand. □

Proposition 4.7. *If N is even, then*

$$\begin{cases} c_{0,N-1} > 0 & \text{if } N \in 4\mathbb{N} \ , \\ c_{0,N-1} < 0 & \text{if } N \in 4\mathbb{N} + 2 \ . \end{cases} \tag{4.34}$$

As a consequence, for $\lambda_1 > 0$ sufficiently small, the system admits exactly $2N$ stationary points on the centre manifold. The points with $\varphi_1 = 2k\pi/N$ have one stable and one unstable direction if $N \in 4\mathbb{N}$, and two stable directions if $N \in 4\mathbb{N} + 2$, and vice versa for the points with $\varphi_1 = (2k + 1)\pi/N$.

Proof: By (4.24), it is sufficient to compute $h_{0m} = h_{m0}$ for odd m between 1 and $N - 3$. Recall that $\lambda_0 = 1$, and $\lambda_k = \lambda_{-k} < 0$ for $3 \leqslant k \leqslant N - 2$. Using $h_{01} = 1$ as starting point, it is easy to show by induction that $\operatorname{sign}(h_{0,2\ell+1}) = (-1)^\ell$, because all summands have the same sign at each iteration. Likewise, all summands of $c_{0,N-1}$ have sign $(-1)^{N/2}$. □

Proof of Theorem 2.3. We consider the case $N = 4L$, the proof being similar for $N = 4L + 2$.

- First note that the set $\mathcal{B} = \{y\colon y_k \in \mathbb{R} \ \forall k\}$ is invariant under the dynamics (it corresponds to $x_{N-j} = x_j \ \forall j$). The intersection of $\mathcal{B}$ with the centre manifold is one-dimensional, and can be parametrised by $r_1 \in \mathbb{R}$ (while $\varphi_1 = 0$). Since $\dot{r}_1 = \lambda_1 r_1 - 3r_1^3 + \mathcal{O}(r_1^4)$, the system admits at least three stationary points O and $\pm B'$ in $\mathcal{B}$ for small positive λ_1. The stationary point B' is stable in the r_1-direction, and unstable in the φ_1-direction. Since there are $N - 3$ stable and 1 unstable directions transversal to the centre manifold, B' is a 2-saddle. The same holds for the cyclic permutations $RB', \dots, R^{N-1}B'$, which correspond to $\varphi_k = 2k\pi/N$, and thus lie in the fixed-point sets of conjugate symmetry groups. Applying the inverse Fourier transformation (4.2), we find that the coordinates of B' in $\mathcal{X}$ satisfy

$$B'_j = \omega^j y_1 + \omega^{-j}\overline{y_1} + \mathcal{O}(\lambda_1) = 2\cos\left(\frac{2\pi j}{N}\right)\sqrt{\frac{\lambda_1}{3}} + \mathcal{O}(\lambda_1) \ . \tag{4.35}$$

  Setting $B = R^{-N/4}B'$ yields the expression (2.23) for the coordinates.
- A similar argument shows the existence of N stationary points $A, RA, \dots, R^{N-1}A$, corresponding to $\varphi_1 = (2k + 1)\pi/N$, which are 1-saddles because they are stable in the φ_1-direction. In $\mathcal{X}$, their coordinates satisfy one of the symmetries $x_{n_0-j} = -x_j$, $n_0 = 1, \dots, N$.

- For λ_1 small enough, the equation $\dot{\varphi}_1 = 0$ admits exactly $2N$ solutions, so that there are no further stationary points on the centre manifold. Proposition 3.1 shows that for any $\eta > 0$, we can find a $\delta > 0$ such that if $\gamma > \gamma_1 - \delta$, there can be no stationary points outside an η-neighbourhood of the diagonal. Together with a local analysis near the diagonal, and the fact that the centre manifold is locally repulsive, this proves that there are exactly $2N + 3$ stationary points.
- Consider now the set

$$\mathcal{A}_+ = \{x \in \mathcal{X} \colon x_j = -x_{N+1-j} = x_{N/2+1-j} \ \forall j,\ x_1, \dots, x_L > 0\} \ . \tag{4.36}$$

  We claim that this set is positively invariant under the flow of $\dot{x} = -\nabla V_\gamma(x)$. Without the condition $x_1, \dots, x_L > 0$, the invariance follows from equivariance. Now if $x_j = 0$ for some j while the other x_i are positive, one easily sees that $-\partial_{x_j} V_\gamma = (x_{j-1} + x_{j+1})\gamma/2$ is positive, showing the invariance of $\mathcal{A}_+$. Since the potential is increasing at infinity, there must be at least one stationary point in $\mathcal{A}_+$, which we denote $A(\gamma)$. As $\gamma \to 0$, the only stationary point in $\mathcal{A}_+$ is the point $(1, \dots, 1, -1, \dots, -1)$. We proceed similarly for $B(\gamma)$.
- Finally, the value of the potential at the stationary points can be computed with the help of the expression (4.4) for the potential in Fourier variables. The only terms contributing to leading order in λ_1 are the term $\lambda_1 |y_1|^2$ in the first sum, and terms of the form $y_1^2 y_{-1}^2$ in the second sum. The remaining terms are of smaller order. The relation on the difference $V_\gamma(B) - V_\gamma(A)$ is a consequence of Remark 4.5. This proves the theorem. □

In the case of odd N, the situation is more difficult, because not all summands in the recursion defining the h_{0m} are of the same sign. A partial result is

Lemma 4.8. *If N is odd, then*

$$\operatorname{sign}(h_{0,2\ell+1}) = (-1)^\ell \qquad \text{for } \ell = 0, 1, \dots, \frac{N-1}{2} - 1 \ . \tag{4.37}$$

Proof: As before, using the fact that $\lambda_k = \lambda_{-k} < 0$ for $1 \leqslant k \leqslant N - 1$. □

Conjecture 4.9. *For $\ell = (N-1)/2, \dots, N-2$, h_{0m} has sign $(-1)^{\ell+1}$, and*

$$c_{0,2N-1} > 0 \ . \tag{4.38}$$

Numerically, we have checked the validity of this conjecture for all odd N up to 101.

Proof of Theorem 2.5. The proof is similar to the above proof of Theorem 2.3, without using any information on the sign of $c_{0,2N-1}$. □

Conjecture 2.6 then follows from Conjecture 4.9 by including the information on the sign of $c_{0,2N-1}$ in the proof.

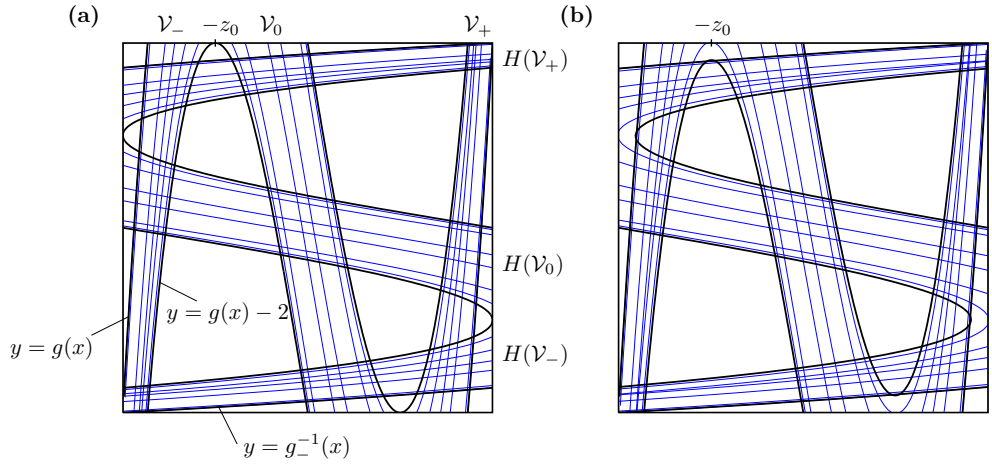

FIGURE 9. Images of the boundary of the square $[-1,1]\times[-1,1]$ under the map H, shown **(a)** for $\gamma = 1/4$, and **(b)** for $\gamma = 0.258\ldots$ The "vertical" strips $\mathcal{V}_-$, $\mathcal{V}_0$ and $\mathcal{V}_+$ are mapped on "horizontal" strips $H(\mathcal{V}_-)$, $H(\mathcal{V}_0)$ and $H(\mathcal{V}_+)$. Their intersections define the elements of the first-level partition, for instance $I_{-,-} = \mathcal{V}_- \cap H(\mathcal{V}_-)$ is the lower-left squarish domain. Intersections of the light curves, obtained by iterating the map twice, define the elements $I_{\omega_{-1}\omega_0.\omega_1\omega_2}$ of the second-level partition.

A Small Coupling and Symbolic Dynamics

In this appendix we sketch the proof of Proposition 2.1 on the continuation of equilibrium points from the uncoupled limit. The equation $f(x_n) + \frac{\gamma}{2}(x_{n+1} - 2x_n + x_{n-1}) = 0$ satisfied by the stationary points of the potential V_γ can be rewritten as $(x_{n+1}, y_{n+1}) = H(x_n, y_n)$ where H is the map of the plane defined by

$$H(x,y) = \left(2x - \frac{2}{\gamma}f(x) - y, x\right). \tag{A.1}$$

This map is invertible and its inverse can be simply obtained as $H^{-1} = S \circ H \circ S$ where $S(x,y) = (y,x)$. In addition, we have $H(-x,-y) = -H(x,y)$.

We proceed to a similar construction as in [Kee87] to show that, when $\gamma \leqslant 1/4$, the map H has an invariant set on which it is conjugated to the full shift with 3 symbols. This implies that the map admits at least 3^N points of (not necessarily minimal) period N for any N. Since the potential V_γ is a polynomial of degree 4 in N variables, it can have at most 3^N stationary points, and thus we will have obtained the exact number of stationary points.

We start by defining a collection of strips in the square $[-1,1]^2$ with good dynamical properties. The map $x \mapsto g(x) \coloneqq 2x - 2\gamma^{-1}f(x) + 1$ leaves -1 invariant and is strictly increasing on $[-1,-z_0]$ where $z_0 \coloneqq \sqrt{(1-\gamma)/3}$. If in addition, the condition $g(-z_0) \geqslant 1$ holds, then g is a bijection on $[-1, g_-^{-1}(1)]$ where g_-^{-1} is the inverse of g with range $[-1,-z_0]$ and we have

$$H\Big(\big\{(x,-1)\colon g_-^{-1}(-1) \leqslant x \leqslant g_-^{-1}(1)\big\}\Big) = \big\{(x, g_-^{-1}(x))\colon -1 \leqslant x \leqslant 1\big\}. \tag{A.2}$$

Similarly, provided that the condition $g(-z_0) \geqslant 3$ is satisfied, we have

$$H\Big(\big\{(x,1)\colon g_-^{-1}(1) \leqslant x \leqslant g_-^{-1}(3)\big\}\Big) = \big\{(x, g_-^{-1}(x+2))\colon -1 \leqslant x \leqslant 1\big\}. \tag{A.3}$$

The condition $g(-z_0) \geqslant 3$ is indeed equivalent to $\gamma \leqslant 1/4$. By monotonicity, it results that under the condition $\gamma \leqslant 1/4$ the "vertical" strip

$$\mathcal{V}_- := \big\{(x,y)\colon g_-^{-1}(y) \leqslant x \leqslant g_-^{-1}(y+2),\ -1 \leqslant y \leqslant 1\big\}\,, \tag{A.4}$$

is mapped onto the "horizontal" strip $S(\mathcal{V}_-)$. By symmetry we also have that $H(\mathcal{V}_+) = S(\mathcal{V}_+)$ where $\mathcal{V}_+ = -\mathcal{V}_-$ is the opposite vertical strip.

Furthermore, g is strictly decreasing on $[-z_0, z_0]$ and the conditions $g(-z_0) \geqslant 1$ and $g(z_0) \leqslant -1$ imply that this map is a bijection on $[g_+^{-1}(1), g_+^{-1}(-1)]$ where g_+^{-1} is the inverse of g with range $[z_0, -z_0]$. The inverse g_+^{-1} has the symmetry $g_+^{-1}(2-x) = -g_+^{-1}(x)$ and the condition $g(z_0) \leqslant -1$ is equivalent to $g(-z_0) \geqslant 3$. Similarly as before this implies that under the condition $\gamma \leqslant 1/4$, the symmetric vertical strip

$$\mathcal{V}_0 := \big\{(x,y)\colon g_+^{-1}(y+2) \leqslant x \leqslant g_+^{-1}(y),\ -1 \leqslant y \leqslant 1\big\}\,, \tag{A.5}$$

is mapped onto the horizontal strip $S(\mathcal{V}_0)$.

With these strips provided, the rest of the construction is standard. Given any finite word $\omega_{-n}\cdots\omega_{n+1} \in \{-,0,+\}^{2(n+1)}$ $(n \geqslant 0)$ consider the set

$$I_{\omega_{-n}\cdots\omega_0.\omega_1\cdots\omega_{n+1}} = \bigcap_{k=-n}^{n+1} H^k(\mathcal{V}_{\omega_k})\,. \tag{A.6}$$

These sets are all non-empty by the properties of the strips above. Then, for any infinite sequence $\{\omega_n\} \in \{-,0,+\}^{\mathbb{Z}}$, the intersection $\bigcap_{k\in\mathbb{Z}} H^k(\mathcal{V}_{\omega_k})$ is also nonempty. Since the sets $I_{\omega_{-n}\cdots\omega_{n+1}}$ are pairwise disjoint, we conclude that the map H has at least (and thus exactly) $3^{\mathbb{Z}}$ points for which the forward and backward orbit is contained in $[-1,1]^2$. In particular it has exactly 3^N points of period N for any N. This shows that $\gamma^\star(N) \geqslant 1/4$ for any $N \geqslant 2$.

The condition $g(-z_0) \geqslant 3$ which ensures that the strips have the desired properties is not optimal and can be improved. To see this, we consider the strips $\mathcal{V}'_{\omega_k}$ instead of $\mathcal{V}_{\omega_k}$ in (A.6) where $\mathcal{V}'_-$ is defined by

$$\mathcal{V}'_- := \big\{(x,y)\colon\ -1 \leqslant x \leqslant -z_0,\ g(x) - 2 \leqslant y \leqslant g(x)\big\}\,, \tag{A.7}$$

where $\mathcal{V}'_+ = -\mathcal{V}'_-$ and where

$$\mathcal{V}'_0 := \big\{(x,y)\colon\ -z_0 \leqslant x \leqslant z_0,\ g(x) - 2 \leqslant y \leqslant g(x)\big\}\,, \tag{A.8}$$

Note that we have $\mathcal{V}'_{\omega_k} \supset \mathcal{V}_{\omega_k}$.

Similarly as before, a sufficient condition for the existence of $3^{\mathbb{Z}}$ points with bounded orbit under H is that the nine basic sets $I_{\omega_0.\omega_1}$ are pairwise disjoint. By symmetries, the latter is equivalent to the condition that the right boundary of $\mathcal{V}'_-$ crosses the upper horizontal strip $S(\mathcal{V}'_+)$. A simple analysis shows that this is equivalent to the inequality (weaker than $g(-z_0) \geqslant 3$)

$$g(-z_0) - 2 \geqslant g_-^{-1}(2 - z_0) \tag{A.9}$$

which holds provided $\gamma \leqslant 0.258\ldots$, i.e., we have $\gamma^\star(N) \geqslant 0.258\ldots$ for any $N \geqslant 2$.

As γ increases, some symbolic sequences will be pruned, resulting in saddle-node bifurcations of stationary points. The first configurations to disappear are asymmetric ones, such as $(1,1,\ldots,1,-1)$ and $(1,1,\ldots,1,0)$ and their images under the symmetry group G.

Orbit label	Fixed-point set	Reduced dynamics
$I^{\pm}$	(x,x,x,x)	$\dot{x} = x - x^3$
A	$(x,x,-x,-x)$	$\dot{x} = (1-\gamma)x - x^3$
B	$(x,0,-x,0)$	$\dot{x} = (1-\gamma)x - x^3$
$A^{(2)}$	$(x,-x,x,-x)$	$\dot{x} = (1-2\gamma)x - x^3$
Aa	(x,x,y,y)	$\dot{x} = (1-\frac{1}{2}\gamma)x + \frac{1}{2}\gamma y - x^3$ $\dot{y} = \frac{1}{2}\gamma x + (1-\frac{1}{2}\gamma)y - y^3$
	(x,y,x,y)	$\dot{x} = (1-\gamma)x + \gamma y - x^3$ $\dot{y} = \gamma x + (1-\gamma)y - y^3$
	$(x,-x,y,-y)$	$\dot{x} = (1-\frac{3}{2}\gamma)x - \frac{1}{2}\gamma y - x^3$ $\dot{y} = -\frac{1}{2}\gamma x + (1-\frac{3}{2}\gamma)y - y^3$
$\partial a, \partial b, \ldots$	(x,y,x,z)	$\dot{x} = (1-\gamma)x + \frac{1}{2}\gamma y + \frac{1}{2}\gamma z - x^3$ $\dot{y} = \gamma x + (1-\gamma)y - y^3$ $\dot{z} = \gamma x + (1-\gamma)z - z^3$

TABLE 6. Orbits, corresponding fixed-point sets and reduced dynamics in the case $N = 4$.

B The case $N = 4$

In this appendix, we briefly describe how we obtained the bifurcation diagram of Figure 5 for the case $N = 4$.

We start by determining the isotropy groups of the stationary points present in the uncoupled case $\gamma = 0$, and their fixed-point sets. They are of 10 different types, 8 of which we show in Table 6. The two types we do not show are the fixed-point set $\{0,0,0,0\}$, which obviously contains only the origin, and the orbits labelled $Aa\alpha$, which have no symmetry, and thus a fixed-point set equal to $\mathcal{X}$.

Table 6 also shows the form taken by the equation $\dot{x} = -\nabla V_\gamma(x)$ when restricted to the fixed-point set. These equations are then analysed in order to determine their equilibrium points. The analysis of the dynamics in one-dimensional fixed-point sets is straightforward, while the two-dimensional equations require a bit more work, but do not present particular difficulties. Let us briefly describe the case of the three-dimensional fixed-point set (x,y,x,z). In rotated variables $u = (y+z)/2$, $v = (y-z)/2$, the equations become

$$\begin{aligned} \dot{x} &= (1-\gamma)x + \gamma u - x^3 \,, \\ \dot{u} &= \gamma x + (1-\gamma)u - u(u^2 + 3v^2) \,, \\ \dot{v} &= (1-\gamma)v - v(3u^2 + v^2) \,. \end{aligned} \tag{B.1}$$

Equilibrium points with $v = 0$ correspond to the fixed-point set (x,y,x,y), and have already been analysed. We thus assume $v \neq 0$, which implies $3u^2 + v^2 = 1 - \gamma$ and allows to eliminate v. We are left with two equations for the stationary points, namely

$$\begin{aligned} (1-\gamma)x + \gamma u - x^3 &= 0 \,, \\ \gamma x - 2(1-\gamma)u + 8u^3 &= 0 \,. \end{aligned} \tag{B.2}$$

If $x = 0$, then necessarily $u = 0$ and we are left with the already studied points of the form $(0, y, 0, -y)$. We thus assume $x \neq 0$ and eliminate u from the system. It is convenient to introduce the variable $w = 2(1 - \gamma - x^2)$ instead of x. Then $u = -wx/2\gamma$, and w has to satisfy the fourth-order equation

$$w^4 - 2(1-\gamma)w^3 + 2\gamma^2(1-\gamma)w + 2\gamma^4 = 0 \,. \tag{B.3}$$

The condition $v^2 \geqslant 0$ yields the additional requirement $w^3 - 2(1-\gamma)w^2 + \frac{8}{3}\gamma^2(1-\gamma) \geqslant 0$. Together with (B.3), this can be seen to be equivalent to the condition

$$\frac{3\gamma^2}{w} \leqslant 1 - \gamma \,. \tag{B.4}$$

Numerically, one observes the following properties:

- If $0 < \gamma < 0.2684\ldots$, Equation (B.3) has four distinct real roots, two of them being positive and two negative.
- For $0.2684\ldots < \gamma < 0.4004\ldots$, Equation (B.3) has two real roots, which are both positive.

The negative roots always fulfil Condition (B.4). Examining (B.3) perturbatively in γ, one finds that they are of the form $w = -\gamma + \mathcal{O}(\gamma^2)$ and $w = -\gamma^2 + \mathcal{O}(\gamma^3)$, and correspond to the branches labelled ∂a and ∂b in the bifurcation diagram of Figure 5.

The positive roots, on the other hand, do not always fulfil Condition (B.4). In fact, one solution exists for $0 < \gamma < (3\sqrt{2} - 2)/7$, while the other one bifurcates with the $A^{(2)}$-branch for $\gamma = 2/5$. A perturbative analysis for small γ shows that they converge, respectively, to the points $(1, 0, 1, -1)$ and $(0, 1, 0, 0)$ as $\gamma \to 0$.

Finally, one can also compute the determinant of the Hessian of the potential around the stationary points of the form (x, y, x, z). This determinant can be put into the form

$$\frac{1}{2w^2}\big[3w - 4(1-\gamma)\big]\big[(1-\gamma)w - 3\gamma^2\big]\big[3(1-\gamma)w^2 + 4(1-2\gamma)w + 6\gamma^2(1-\gamma)\big] \,. \tag{B.5}$$

The roots of this expression correspond to bifurcation points, and can be combined with (B.3) to check that all bifurcation points have been found (and yields more precise estimates of the bifurcation values). This expression can also be used to check the index of the stationary points.

This analysis is not completely rigorous because we have not analysed in detail the branch labelled $Aa\alpha$, which has no symmetry at all. The bifurcation diagram is based on the fact that the only bifurcation of already known branches producing stationary points without symmetry is the bifurcation of the Aa-branch at $\gamma = 1/3$. A local analysis shows that this is indeed a pitchfork bifurcation, producing the right number of new stationary points.

References

[AS92] P. Ashwin and J. W. Swift, *The dynamics of n weakly coupled identical oscillators*, J. Nonlinear Sci. **2** (1992), no. 1, 69–108.

[BEGK04] Anton Bovier, Michael Eckhoff, Véronique Gayrard, and Markus Klein, *Metastability in reversible diffusion processes. I. Sharp asymptotics for capacities and exit times*, J. Eur. Math. Soc. (JEMS) **6** (2004), no. 4, 399–424.

[BFG06b] Nils Berglund, Bastien Fernandez, and Barbara Gentz, *Metastability in interacting nonlinear stochastic differential equations II: Large-N behaviour*, Preprint, 2006.

[BGK05] Anton Bovier, Véronique Gayrard, and Markus Klein, *Metastability in reversible diffusion processes. II. Precise asymptotics for small eigenvalues*, J. Eur. Math. Soc. (JEMS) **7** (2005), no. 1, 69–99.

[BM96] Vladimir N. Belykh and Erik Mosekilde, *One-dimensional map lattices: synchronization, bifurcations, and chaotic structures*, Phys. Rev. E (3) **54** (1996), no. 4, part A, 3196–3203.

[CF05] J.-R. Chazottes and B. Fernandez, *Dynamics of coupled map lattices and of related spatially extended systems*, Lecture Notes in Physics, vol. 671, Springer-Verlag., New York, 2005.

[CMPVV96] Shui-Nee Chow, John Mallet-Paret, and Erik S. Van Vleck, *Dynamics of lattice differential equations*, Proceedings of the Workshop on Discretely-Coupled Dynamical Systems, Part I (Santiago de Compostela, 1995), vol. 6, 1996, pp. 1605–1621.

[DG88] D. A. Dawson and J. Gärtner, *Long time behaviour of interacting diffusions*, Stochastic calculus in application (Cambridge, 1987), Pitman Res. Notes Math. Ser., vol. 197, Longman Sci. Tech., Harlow, 1988, pp. 29–54.

[DGS96a] Benoit Dionne, Martin Golubitsky, and Ian Stewart, *Coupled cells with internal symmetry. I. Wreath products*, Nonlinearity **9** (1996), no. 2, 559–574.

[DGS96b] ———, *Coupled cells with internal symmetry. II. Direct products*, Nonlinearity **9** (1996), no. 2, 575–599.

[dH04] F. den Hollander, *Metastability under stochastic dynamics*, Stochastic Process. Appl. **114** (2004), no. 1, 1–26.

[EH01] J.-P. Eckmann and M. Hairer, *Uniqueness of the invariant measure for a stochastic PDE driven by degenerate noise*, Comm. Math. Phys. **219** (2001), no. 3, 523–565.

[EN93] Thomas Erneux and Grégoire Nicolis, *Propagating waves in discrete bistable reaction-diffusion systems*, Phys. D **67** (1993), no. 1-3, 237–244.

[EPRB99] J.-P. Eckmann, C.-A. Pillet, and L. Rey-Bellet, *Non-equilibrium statistical mechanics of anharmonic chains coupled to two heat baths at different temperatures*, Comm. Math. Phys. **201** (1999), no. 3, 657–697.

[FKM65] G. W. Ford, M. Kac, and P. Mazur, *Statistical mechanics of assemblies of coupled oscillators*, J. Mathematical Phys. **6** (1965), 504–515.

[FM96] L. Floria and J. Mazo, *Dissipative dynamics of the Frenkel-Kontorova model*, Adv. Phys. **45** (1996), 505–598.

[FW98] M. I. Freidlin and A. D. Wentzell, *Random perturbations of dynamical systems*, second ed., Springer-Verlag, New York, 1998.

[Joh97] Mark E. Johnston, *Bifurcations of coupled bistable maps*, Phys. Lett. A **229** (1997), no. 3, 156–164.

[Kee87] James P. Keener, *Propagation and its failure in coupled systems of discrete excitable cells*, SIAM J. Appl. Math. **47** (1987), no. 3, 556–572.

[Kif81] Yuri Kifer, *The exit problem for small random perturbations of dynamical systems with a hyperbolic fixed point*, Israel J. Math. **40** (1981), no. 1, 74–96.

[Kol00] Vassili N. Kolokoltsov, *Semiclassical analysis for diffusions and stochastic processes*, Lecture Notes in Mathematics, vol. 1724, Springer-Verlag, Berlin, 2000.

[McN99] Ken McNeil, *Bifurcations in ring arrays of phase-bistable systems*, Internat. J. Bifur. Chaos Appl. Sci. Engrg. **9** (1999), no. 1, 107–117.

[McN02] ———, *Bifurcations and clustering in globally coupled arrays of phase-bistable systems*, Internat. J. Bifur. Chaos Appl. Sci. Engrg. **12** (2002), no. 2, 309–318.

[NMKV97] V. I. Nekorkin, V. A. Makarov, V. B. Kazantsev, and M. G. Velarde, *Spatial disorder and pattern formation in lattices of coupled bistable elements*, Phys. D **100** (1997), no. 3-4, 330–342.

[OV05] Enzo Olivieri and Maria Eulália Vares, *Large deviations and metastability*, Encyclopedia of Mathematics and its Applications, vol. 100, Cambridge University Press, Cambridge, 2005.

[PRK01] Arkady Pikovsky, Michael Rosenblum, and Jürgen Kurths, *Synchronization, a universal concept in nonlinear sciences*, Cambridge Nonlinear Science Series, vol. 12, Cambridge University Press, Cambridge, 2001.

[QC04] Wen-Xin Qin and Yihui Chen, *Bifurcations and persistence of equilibria in high-dimensional lattice dynamical systems*, Nonlinearity **17** (2004), no. 2, 519–539.

[RBT00] Luc Rey-Bellet and Lawrence E. Thomas, *Asymptotic behavior of thermal nonequilibrium steady states for a driven chain of anharmonic oscillators*, Comm. Math. Phys. **215** (2000), no. 1, 1–24.

[RBT02] ———, *Exponential convergence to non-equilibrium stationary states in classical statistical mechanics*, Comm. Math. Phys. **225** (2002), no. 2, 305–329.

[Rou02] Jacques Rougemont, *Space-time invariant measures, entropy, and dimension for stochastic Ginzburg-Landau equations*, Comm. Math. Phys. **225** (2002), no. 2, 423–448.

[SL77] Herbert Spohn and Joel L. Lebowitz, *Stationary non-equilibrium states of infinite harmonic systems*, Comm. Math. Phys. **54** (1977), no. 2, 97–120.

[Sug96] Makoto Sugiura, *Exponential asymptotics in the small parameter exit problem*, Nagoya Math. J. **144** (1996), 137–154.

[Wat93a] Masaji Watanabe, *Bifurcation of synchronized periodic solutions in systems of coupled oscillators. I. Perturbation results for weak and strong coupling*, Rocky Mountain J. Math. **23** (1993), no. 4, 1483–1525.

[Wat93b] ———, *Bifurcation of synchronized periodic solutions in systems of coupled oscillators. II. Global bifurcation in coupled planar oscillators*, Rocky Mountain J. Math. **23** (1993), no. 4, 1527–1554.

Nils Berglund
CPT–CNRS Luminy
Case 907, 13288 Marseille Cedex 9, France
and
PHYMAT, Université du Sud Toulon–Var
Present address:
MAPMO–CNRS, Université d'Orléans
Bâtiment de Mathématiques, Rue de Chartres
B.P. 6759, 45067 Orléans Cedex 2, France
E-mail address: berglund@cpt.univ-mrs.fr

Bastien Fernandez
CPT–CNRS Luminy
Case 907, 13288 Marseille Cedex 9, France
E-mail address: fernandez@cpt.univ-mrs.fr

Barbara Gentz
Weierstrass Institute for Applied Analysis and Stochastics
Mohrenstraße 39, 10117 Berlin, Germany
Present address:
Faculty of Mathematics, University of Bielefeld
P.O. Box 10 01 31, 33501 Bielefeld, Germany
E-mail address: gentz@math.uni-bielefeld.de